Contents lists available at ScienceDirect

Environmental and Experimental Botany

journal homepage: www.elsevier.com/locate/envexpbot

Limited Zn supply affects nutrient distribution, carbon metabolism and causes nitro-oxidative stress in sensitive *Brassica napus*

Arpád Molnár [a], Selahattin Kondak [a,b], Péter Benkő [b,c], Patrick Janovszky [d], Kamilla Kovács [a], Réka Szőllősi [a], Orsolya Kinga Gondor [e], Dóra Oláh [a,b], Katalin Gémes [a,c], Gábor Galbács [d], Tibor Janda [e], Zsuzsanna Kolbert [a,*]

[a] *Department of Plant Biology, University of Szeged, Közép fasor 52, 6726 Szeged, Hungary*
[b] *Doctoral School of Biology, Faculty of Science and Informatics, University of Szeged, Közép fasor 52, 6726 Szeged, Hungary*
[c] *Institute of Plant Biology, Biological Research Centre, Eötvös Loránd Research Network, Temesvári krt 62, 6726 Szeged, Hungary*
[d] *Department of Inorganic and Analytical Chemistry, University of Szeged, Dóm tér 7, 6720 Szeged, Hungary*
[e] *Agricultural Institute, Centre for Agricultural Research, Eötvös Loránd Research Network, Brunszvik utca 2, 2462 Martonvásár, Hungary*

ARTICLE INFO

ABSTRACT

Despite being a worldwide problem, responses of crops to zinc (Zn) deficiency is largely unknown. This study examines the effects of limited Zn supply in *Brassica napus*. The decreased Zn content of the nutrient solution caused reduced tissue Zn concentrations and reduced K, Ca, Mg levels were detected in the leaves. For Ca, Zn, Fe, Mo inhomogeneous distribution was induced by Zn limitation. Suboptimal Zn supply decreased the shoot and root biomass and altered the root structure. The levels of sugars and sugar phosphates (e.g. glucose, glucose-6-phosphate etc.) were decreased suggesting disturbance in carbon metabolism. Limited Zn availability induced organ-dependent superoxide anion and hydrogen peroxide production and triggered altered NADPH oxidase, superoxide dismutase activities, ascorbate peroxidase abundance and ascorbate and glutathione contents indicating oxidative stress. Moreover, nitric oxide, peroxynitrite and S-nitrosoglutathione (GSNO) levels and GSNO reductase gene expression, protein level and activity were modified by Zn limitation. As a consequence, protein tyrosine nitration and protein carbonylation were intensified in *B. napus* grown with suboptimal Zn supply. Collectively, these results provide the first evidence for Zn deficiency-induced imbalances in nutrient status, sugar contents, reactive oxygen and nitrogen species metabolisms and for the secondary nitro-oxidative stress in sensitive *Brassica napus*.

1. Introduction

Zinc (Zn) is a trace metal that is essential for prokaryotic and eukaryotic organisms, including plants, due to its essential biological roles (Cakmak, 2000; Hänsch and Mendel, 2009).

Zn is a cofactor in plant proteins (e.g. carbonic anhydrase, Cu/Zn superoxide dismutase [SOD], alcohol dehydrogenase) and is a structural element in zinc finger transcription factors, membrane lipids, and DNA/RNA. Hence, the maintenance of optimal Zn concentration in metabolically active plant tissues determines protein metabolism, gene expression and membrane integrity (Broadley et al., 2007).

Zinc required by plants derives primarily from the soil, where Zn^{2+} accounts for up to 50% of the soluble Zn fraction (Cakmak, 2002; Hacisalihoglu and Kochian, 2003, Noulas et al., 2018). The availability of Zn for plant uptake may be limited due to several influencing factors (low Zn concentrations, high pH, high phosphorus content, flooding etc.) and under such circumstances plants may suffer from the consequences of Zn deficiency (Noulas et al., 2018). Regarding to the perception of Zn deficiency by plants, results obtained in Arabidopsis model show that the bZIP19 and bZIP23 transcription factors bind Zn^{2+} ions to a Zn-sensor motif thus acting like sensor elements in Zn deficiency response (Lilay et al., 2021).

In general, for the majority of crops the optimal Zn level is between 30 and 200 μg Zn/g dry weight (Marschner, 2012). Among crops, rice, maize and grapes are highly sensitive to low Zn supply, whereas pea, carrot and alfalfa are tolerant species (Alloway, 2008; Thiébaut and Hanikenne, 2022). Plant species sensitive to inadequate Zn supply show symptoms like stunted organ growth, chlorosis, limited leaf growth or

---

spikelet sterility even as the effect of short-term Zn limitation. Low Zn supply intensifies the susceptibility of plants to biotic or abiotic stress factors (Ullah et al., 2019; Cabot et al., 2019). Inadequate Zn availability negatively affects the capacity for water uptake and transport and also the synthesis of tryptophan which is a precursor of indole-acetic-acid (IAA) resulting in inadequate production of this phytohormone (Thiébaut and Hanikenne, 2022). Furthermore, deficiency in Zn supply induces increased formation of reactive oxygen species (ROS) like superoxide anion radical ($O_2^{\bullet-}$) and hydrogen peroxide (H_2O_2) by activating their enzymatic production and limiting enzymatic detoxification via inhibiting the activity or gene expression of e.g. SOD, ascorbate peroxidase (APX), glutathione reductase (GR), peroxidases (POX) (Cakmak and Marschner, 1988; Cakmak, 2000; Zeng et al., 2019a,b; Shinozaki et al., 2020; Zeng et al., 2021; Thiébaut and Hanikenne, 2022). A change in the amount of non-enzymatic antioxidants, mainly ascorbate and glutathione is also associated with Zn deficiency (Höller et al., 2014; Tewari et al., 2019), and the imbalance in the formation and elimination of ROS leads to oxidative modifications affecting nucleic acids, lipids and proteins. Of the several ROS-related post-translational modifications, carbonylation involves the introduction of carbonyl groups into protein side chains of lysine, proline and threonine via the Fenton reaction or prompting the generation of α,β-unsaturated aldehydes, which form carbonyl adducts on cysteine, histidine, and lysine side chains in a non-enzymatic process (Johansson et al., 2004; Tola et al., 2021). As a result of protein carbonylation, the proteins lose their activity and are designated for proteasomal degradation by the 20 S proteasome (Gili and Sharon, 2014) or highly carbonylated proteins may aggregate in the cytoplasm causing cytotoxicity (Nystrom, 2005; Tola et al., 2021).

Plant cells also produce reactive nitrogen species (RNS) including, inter alia, nitric oxide (NO), nitrogen dioxide radical ($NO_2^{\bullet}$), peroxynitrite ($ONOO^-$) and *S*-nitrosoglutathione (GSNO) (Corpas et al., 2007). Nitric oxide signal is perceived mainly at the level of the proteome through NO-dependent post-translational modifications (PTMs) (Neill et al., 2008; Umbreen et al., 2018).

The GSNO molecule is the primer substance mediating protein *S*-nitrosation. This NO-related PTM reversibly affects cysteine (Cys) residues due to the formation of SNO groups causing activation or inactivation of certain target proteins (Hess et al., 2005). The level of GSNO thus the intensity of NO signalling is regulated by GSNO reductase (GSNOR), which catalyses the NADH-dependent reduction of GSNO to glutathione disulfide and ammonia (Jahnová et al., 2019; Ventimiglia and Mutus, 2020). The enzyme belongs to the class III alcohol dehydrogenase family (Martinez et al., 1996) and it is a homodimer containing two Zn atoms as cofactors per subunit (Kubienova et al., 2013; Lindermayr, 2018). The enzyme is rich in Cys residues which coordinate structural and catalytic Zn atoms (Lindermayr, 2018).

In addition to ROS-dependent protein carbonylation, stress-induced proteome remodelling can also be accomplished through protein nitration. During the irreversible reaction, $NO_2^{\bullet}$ derived from $ONOO^-$ reacts mainly with tyrosine (Tyr) amino acids and as a consequence, a nitro-group is attached to the aromatic ring of Tyr yielding 3-nitrotyrosine inducing structural and functional modification in the protein. Tyrosine nitration causes activity loss and possibly assigns plant proteins for proteasomal degradation (Kolbert et al., 2017; Corpas et al., 2021). Through the above molecular mechanisms, NO regulates multiple physiological processes associated with abiotic stress responses (Fancy et al., 2017). It is widely reported that NO is an integral regulator of stress responses of plants to limited supply of nutrients like nitrogen, phosphorus or iron (Buet et al., 2019), but our knowledge about the role of NO signaling in Zn-deprived plants is very limited (Kondak et al., 2022).

Despite its economic importance, Zn deficiency responses have not been yet evaluated at the molecular level in oilseed rape (*Brassica napus*) (Billard et al., 2015). Furthermore, bridging the gap between Arabidopsis and closely relative dicot crops, like *Brassica napus,* is an urgent task (Thiébaut and Hanikenne, 2022). The lack of knowledge prompted

us to evaluate the Zn deficiency tolerance of *Brassica napus* by determining biomass production and tissue Zn levels. Furthermore, our aim was to provide the first evidences for the Zn-deficiency induced changes in nutrient composition and sugar/sugar phosphate levels, endogenous ROS and RNS metabolism and oxidative and nitrosative protein modifications in this important crop species.

2. Materials and methods

2.1. Plant material and growing

Experiments were carried out using oilseed rape (*Brassica napus* L. cv. GK Gabriella). Seeds were surface-sterilized (70 v/v % ethanol of 1 min followed by 5% v/v sodium hypochlorite for 15 min) and placed in Petri-dishes containing filter paper moistened with distilled water. After 9 days, seedlings having three real leaves were transferred to a plastic foam floating on the surface of full or Zn-deprived modified Hoagland solution being optimal for the hydroponic cultivation of *Brassica napus*. The nutrient solution was aerated in order to avoid anoxia. The full solution contained 5 mM $Ca(NO_3)_2$, 5 mM KNO_3, 2 mM $MgSO_4$, 1 mM KH_2PO_4, 0.01 mM Fe-EDTA,10 μM H_3BO_3, 1 μM $MnSO_4$, 5 μM $ZnSO_4$, 0.5 μM $CuSO_4$, 0.1 μM $(NH_4)_6Mo_7O_{24}$ and 10 μM $CoCl_2$. Based on pilot experiments, we chose Zn/10 (zinc content reduced by one tenth) as a Zn deficiency treatment which induced physiological, biochemical and gene expression responses but didn't cause plant death. The zinc deficient nutrient solution was prepared by adding 0.5 μM $ZnSO_4$. The actual zinc ion concentration in full nutrient solution was 47.3 μg/L, while Zn deprived solution contained 3.8 times less (12.2 μg/L) Zn. Zinc concentrations in the solutions were determined by inductively coupled plasma optical emission spectrometry (ICP-OES). Plants were grown in full or Zn deficient (Zn/10) nutrient solutions for three weeks under controlled conditions (150 μmol/m^{-2}/s photon flux density with 12 h/ 12 h light/dark cycle, relative humidity 55–60% and temperature 25 ± 2 °C).

2.2. Analysis of in planta Zn and Fe contents

Roots and shoots of *Brassica napus* were harvested separately and washed in distilled water then dried at 70 °C for 72 h. Dried plant material (100 mg) was incubated with nitric acid (6 ml, 65% w/v, Reanal, Hungary) for 2 h, and with hydrogen peroxide (2 ml, 30%, w/v, VWR Chemicals, Hungary). The samples were destructed at 200 °C and 1600 W for 15 min. The zinc and iron concentrations of leaf and root samples were determined by inductively coupled plasma mass spectrometry (Agilent 7700 Series, Santa Clara, USA) and the data are given in μg/g dry weight (DW).

In situ levels of free, intracellular Zn^{2+} were estimated by using Zinquin fluorophore in the root tips. Samples were incubated in 1 x PBS (pH 7.4) and then stained with 25 μM Zinquin (prepared in 1x PBS buffer) for 60 min at room temperature in the dark. Samples were prepared on slides following washing in PBS buffer (Sarret et al., 2006).

2.3. Calculations of Zn deficiency tolerance parameters

Zinc deficiency tolerance index (%) was determined by using the following equation (Ghandilyan et al., 2012):

$$\frac{shoot\ dry\ weight\ under\ Zn\ deficient\ condition}{shoot\ dry\ weight\ under\ Zn\ sufficient\ condition} \times 100$$

Zinc efficiency was determined using the following equation (Ghandilyan et al., 2012):

$$\frac{shoot\ Zn\ concentration\ under\ Zn\ deficiency\ condition}{shoot\ Zn\ concentration\ under\ Zn\ sufficient\ condition}$$

Zinc usage index was calculated using the following formula (Campos et al., 2017):

$$\frac{shoot \quad fresh \quad biomass \quad (mg)}{shoot \quad Zn \quad concentration \quad (ppm)}$$

2.4. Analysis of macro- and microelement distributions in Brassica leaves by laser-induced breakdown spectroscopy (LIBS)

Fully expanded leaves of *Brassica napus* were pressed, dried for 5 days and mounted on a glass microscope slide with a double-sided foam tape. LIBS experiments were performed on a J-200 tandem LA/LIBS instrument (Applied Spectra, USA), in the LIBS mode. This instrument is equipped with a 266 nm, 6 ns Nd:YAG laser source and a six-channel CCD spectrometer with an optical resolution of 0.07 nm. For every laser shot, the full LIBS spectra over the wavelength range of 190–1040 nm were recorded in the Axiom data acquisition software, using a 0.5 μs gate delay and 1 ms gate width. During the experiments, a 100 μm laser spot size was maintained. The scan was performed in step mode, without overlaps in the laser spots. The pulse energy was generally set at 12 mJ and the laser repetition frequency was 7 Hz. The number of repeated measurements in one sampling location (without translation) was one. During the elemental LIBS mapping of each sample, more than 14000 spectra were collected in an area of 20×15 mm (Limbeck et al., 2021).

2.5. Analysis of biomass production, root architecture and cell viability

Following shoot and root fresh weight measurement using an analytical scale, the plant material was dried at 70 ℃ for 72 h and weighted again. Primary root length was measured and lateral root number was counted manually.

Cell viability was determined by using fluorescein diacetate (FDA) fluorophore. Root tips were incubated with 10 μM FDA solution in MES buffer (10/50 mM MES/KCl, pH 6.15) for 30 min in the dark and were washed four times with the same buffer. Viability of the root tip tissue was expressed in percentage of the fluorescent intensity measured in control samples.

2.6. Metabolomics analysis of amino acids, sugars and sugar derivatives

The Shimadzu GCMS-TQ8040 sample preparation is based on Gondor et al. (2021) with modifications. Plant samples were extracted after the internal standard was added (Adonitol 60 μL of 1 mg ml^{-1} solution). The preparation of the leaf and root samples were performed the mentioned way. The samples were injected in split mode to the Shimadzu GCMS-TQ8040 at 230 ℃. 1 μL of derivatized sample was injected to GCMS-TQ8040 was equipped with 30 m column (HP-5MS ui 30 m, 0.25 mm, 0.25 μm), the carrier gas (He) was used at constant flow rate (1 ml min^{-1}). The thermal program started with 50 ℃ for 1 min and increased to 320 ℃ for 3 min in 7 ℃ min^{-1}. Data evaluation was performed LabSolution GCMS solution Version 4.45 used analytical standard and Finn and Nist version 2.3 databases.

2.7. Detection of ROS and RNS levels in leaves and roots by microscopic methods

In fully-expanded Brassica leaves, nitro blue tetrazolium (NBT) was used for visualizing superoxide production. Excised leaves were incubated in Falcon tubes containing 25 ml of NBT solution (0.2% (w/v) in 50 mM phosphate buffer, pH 7.4) overnight in darkness. Pigments were removed by incubating the leaves in 96% (v/v) ethanol at 70 ℃ for 10 min (Kumar et al., 2014).

For the visualisation of H_2O_2, leaves were incubated in 3,3′-diaminobenzidine (DAB) solution (1 mg/ml prepared in distilled water, 3.8 pH with HCl) overnight in darkness. Pigments were removed with boiling the leaves in 96% (v/v) ethanol for 10 min (Kumar et al., 2014).

Dihydroethidium (DHE, 10 μM) was applied for the detection of superoxide anion levels in the roots. Root segments were incubated for 30 min in the dark at room temperature, and washed twice with Tris–HCl buffer (10 mM, pH 7.4).

Hydrogen peroxide was visualized in root tips using Amplex Red (AR). Samples were incubated in 50 μM AR solution (prepared in sodium phosphate buffer pH 7.5) for 30 min at room temperature in the dark. The microscopic analysis was preceded by one washing step with sodium phosphate buffer.

The nitric oxide levels of the root tips and hand-made cross-sections of fully-expanded leaves were monitored with the help of 4-amino-5-methylamino-2′,7′-difluorofluorescein diacetate (DAF-FM DA). To ensure the absence of gases and even distribution of fluorophore in leaves, cross sections were infiltrated with buffer before staining during all methods. Samples were incubated in 10 μM dye solution for 30 min (darkness, 25 ± 2 ℃) and washed twice with Tris–HCl (10 mM, pH 7.4).

Peroxynitrite was also visualized in root tips and in handmade cross-sections of fully-expanded leaves. Samples were incubated in 10 μM aminophenyl fluorescein (APF) prepared in Tris–HCl buffer. After 30 min of incubation at room temperature, root tips and leaf segments were washed twice with the buffer solution.

For immunodetection, small pieces of root samples derived from the mature zone were fixed in 4% (w/v) paraformaldehyde. After the fixation, root samples were washed in distilled water and embedded in 5% agar (bacterial). Then 100 μm thick cross-sections were prepared using a vibratome (VT 1000 S, Leica) and immunodetection was performed according to Corpas et al. (2008) with slight modifications. Free-floating sections were incubated at room temperature overnight with rat antibody against GSNO (VWR Chemicals) diluted 1:2500 in TBSA–BSAT solution containing 5 mM Tris buffer (pH 7.2), 0.9% (w/v) NaCl, 0.05% (w/v) sodium azide, 0.1% (w/v) BSA and 0.1% (v/v) Triton X-100. Samples were washed three times with TBSA–BSAT solution within 15 min. Following the washing steps, samples were labelled with fluorescein isothiocyanate (FITC)-conjugated rabbit anti-rat IgG secondary antibody (1:1000 in TBSA–BSAT, Agrisera) for 1 h at room temperature. Samples were placed on microscopic slides in phosphate-buffered saline (PBS):glycerine (1:1). In leaves, GSNO immunohistochemistry has been carried out similar to roots using hand-made cross-sections. Samples were infiltrated with buffer for optimal staining conditions.

All microscopy measurements were carried out under Zeiss Axiovert 200 M inverted microscope (Carl Zeiss, Jena, Germany) equipped with a digital camera (AxiocamHR, HQ CCD, Carl Zeiss, Jena, Germany). Filter set 10 (exc.: 450–490, em.: 515–565 nm) was used for FDA, DAF-FM, APF and FITC, filter set 9 (exc.:450–490 nm, em.:515–∞ nm) for DHE, filter set 20HE (exc.: 546/12 nm, em.: 607/80 nm) for AR. Axiovision Rel. 4.8 software (Carl Zeiss, Jena, Germany) was applied for measuring of the pixel intensity on digital photographs.

2.8. Protein extraction and analysis of NOX and SOD isoenzyme activity by native-PAGE

Shoot and root of *Brassica napus* were ground with double volume of extraction buffer (50 mM Tris–HCl buffer pH 7.6–7.8) containing 0.1 mM EDTA, 0.1% Triton X-100% and 10% glycerol and centrifuged at $9300 \times g$ for 20 min at 4 ℃. The protein extract was treated with 1% protease inhibitor cocktail and stored at −20 ℃. Protein concentration was measured with bovine serum albumin as a standard (Bradford, 1976).

For the detection of NOX activity, 10 μg of extracted proteins were subjected to 10 (w/v)% native gel electrophoresis. For the visualisation of the enzyme activity gels were incubated in a Tris-HCl buffer (10 mM pH 7.4) with 0.2 mM NADPH and 0.2 mM NBT. NOX activity was confirmed using DPI.

To visualise SOD isoenzymes, protein extract containing 10 μg protein was separated on 10 (w/v)% native polyacrylamide gel. Gels were incubated in 2.45 mM NBT for 20 min and 28 mM TEMED containing 2.92 μM riboflavin for 15 min in darkness (both solutions were prepared

in 50 mM phosphate buffer pH 7.8). Following two washing steps, gels were developed in light. To identify different isoenzymes, 2 mM KCN was used to inhibit Cu/Zn SOD isoforms and 5 mM H_2O_2 was used to inhibit Cu/Zn and Fe SOD isoforms, respectively.

2.9. Analysis of SOD activity, ascorbate and glutathione levels and GSNOR activity by spectrophotometry

For SOD activity, 250 mg of plant tissues were grounded with 1 ml of extraction buffer (50 mM phosphate buffer pH 7.0 with 1 mM EDTA and 4 (w/v)% PVPP). The activity was measured based on the ability of SODs to inhibit the reduction of NBT to formazan under light (Dhindsa et al., 1981). Data are shown as unit/g fresh weight, where 1 unit is equivalent to 50% inhibition of NBT reduction. The enzyme activity is expressed as unit/g fresh weight; 1 unit of SOD corresponds to the amount of enzyme causing a 50% inhibition of NBT reduction in light.

For quantifying ascorbate and glutathione content, root and shoot material was grounded with 5% trichloroacetic acid and centrifuged (20 min, 9300 g, 4 °C) and the supernatant was used. For the determination of reduced (AsA_{red}) and oxidized (AsA_{ox}) ascorbate content the method of Law et al. (1983) was used which is based on the reduction of Fe^{3+} to Fe^{2+} by ascorbate. AsA_{red}/AsA_{ox} contents are expressed in µmol/g fresh weight. The measurement of the content of reduced (GSH_{red}) and oxidized (GSH_{ox}) glutathione was performed according to the method of Griffith (1980). Data are shown as nmol/g fresh weight.

The GSNOR activity was determined by monitoring NADH oxidation in the presence of GSNO at 340 nm (Sakamoto et al., 2002). Plant homogenate was centrifuged at $9300 \times g$ for 20 min at 4 °C and 150 µL of protein extract was incubated in 1 ml reaction buffer containing 20 mM Tris–HCl pH 8.0, 0.5 mM EDTA, 0.2 mM NADH and 0.4 mM GSNO. Data are expressed as nmol NADH/min/mg protein.

2.10. Analysis of gene expression by qRT-PCR

RNA was extracted from *B. napus* root and shoot samples frozen at − 80 °C. Following grinding the samples in liquid nitrogen, RNA extraction was performed by Quick-RNA Miniprep Kit (Zymo Research, Irvine, CA, USA) according to the manufacturer's instructions. To evaluate the quality and quantity of isolated RNA NanoDrop™2000/ 2000c spectrophotometer (Thermo Fisher Scientific, Waltham, MA, USA) was used. For cDNA synthesis, 1 µg of total RNA was reverse-transcribed using RevertAidFirst Strand cDNA Synthesis Kit (Thermo Fisher Scientific) according to the manufacturer 's instructions. Primers were designed using NCBI primer design tool (Ye et al., 2012). Primer sequences are shown in Table S1. Quantitative reverse transcription (qRT)-PCR was performed using CFX384 Touch Real-Time PCR Detection System (Bio-Rad Laboratories Inc., Hercules, CA, USA) to determine Relative mRNA levels from 1:10 diluted cDNA. As reference gene, *BnActin7* (Bra028615) was used. The RT-qPCR reactions were carried out in a total volume of 7 µL. The PCR mixture contained 1 µL cDNA, 0.21 µL forward and reverse primers 3.5 µL Maxima SYBR Green/ROX qPCR MasterMix (2 ×) (Thermo Fisher Scientific). Reaction mixture was aliquoted to Hard-Shell®384-well plates (thin-wall, skirted, white; Bio-Rad, Cat. no: HSP3805). For amplification, a standard two-step thermal cycling profile was used (10 s at 95 °C and 1 min at 60 °C) up to 40 cycles following a 15 min preheating step at 95 °C. Finally, a dissociation stage was added at 95 °C for 15 s, 60 °C for 15 s, and 95 °C for 15 s. Data analysis was performed using Bio-Rad CFX Maestro (Bio-Rad) software and Microsoft Office Excel 2016. The $2^{-\Delta\Delta Ct}$ method was used for calculating relative mRNA levels.

2.11. Analysis of protein abundance of APX and GSNOR by western blot

Protein extracts were prepared as described above. Denaturated protein extract (15 µg for GSNOR, 10 µg for APX) was subjected to SDS-PAGE (12%). Following the wet blotting (25 mA, 16 h) membranes were used for cross reactivity assays using different antibodies. Loading controls were performed using anti-actin antibody (Agrisera, cat. No. AS13 2640) and as protein standard actin (from bovine muscle, Sigma-Aldrich, cat. No. A3653) was used.

Immunoassays for GSNOR and APX enzymes were performed using polyclonal primary antibodies from rabbit (anti-GSNOR, Agrisera, cat. No. AS09 647 anti-APX, Agrisera, cat. No. AS 08 368,) and affinity-isolated goat anti-rabbit IgG–alkaline phosphatase secondary antibody (Sigma-Aldrich, cat. No. A3687, 1:10 000). The procedures are described in Kolbert et al. (2018).

2.12. Analysis of protein nitration and carbonylation by western blot

Protein extracts were prepared as described earlier. To evaluate The electrophoresis and transfer was evaluated using Coomassie Brilliant Blue R-350 according to Welinder and Ekblad (2011). Actin from bovine liver (Sigma-Aldrich, cat. No. A3653) was used as a protein standard. We performed silver staining as previously described.

A 15 µg aliquot of denaturated root and shoot protein was subjected to SDS–PAGE on 12% acrylamide gels. The proteins were transferred to PVDF membranes (25 mA, 16 h) and the membranes were used for cross-reactivity assays with rabbit polyclonal antibody against 3-nitro-tyrosine (Sigma-Aldrich, cat. No. N0409, 1:2000 diluted). Affinity-isolated goat anti-rabbit IgG–alkaline phosphatase secondary antibody at a dilution of 1:10000 was used for immunodetection. Protein bands were visualized by by the NBT/BCIP (5-bromo-4-chloro-3-indolyl phosphate) reaction. Nitrated BSA served as positive control.

Carbonyl groups added to proteins during oxidative reactions were examined with Abcam's oxidized protein assay kit (ab 178020) with slight modifications to the manufacturer's instructions. Plant biomass was homogenized with 50 mM DTT containing extraction buffer. Samples were incubated on ice for 20 min, then centrifuged at 18 000 g for 20 min on 4 °C. Protein concentration was measured with Bradford protein assay. Two aliquots (10 µL each) were used for the derivation reaction. First aliquot was incubated with 10 µL 12% SDS and 20 µL 1x DNPH solution. The reaction was stopped after 15 min with 20 µL neutralization solution and was ready for gel electrophoresis. In case of the negative control, instead of 1x DNPH solution 20 µL of 1x derivation control solution was added. 7.5 µg of derivatized or derivatisation control protein samples were loaded with loading buffer into wells, SDS-PAGE and membrane transfer was performed as described above. Membranes were blocked for 1 h in buffer (1 × PBS, pH 7,5 with 0.05% Tween 20% and 5% non-fat milk) and assayed with 1 × primary anti-DNP antibody (1:5000) for 3 h at room temperature. Membranes were washed three times with 1 × PBS-T, then secondary antibody assay was performed with goat anti-rabbit IgG–alkaline phosphatase secondary antibody (1:10000). Signal development was performed similar to the previous method, using the manufacturer's DNP-labelled protein as positive control.

2.13. Statistical analysis

Results are shown as mean values of raw data (± SE or ± SD). For statistical analysis, Student's *t*-test or Duncan's multiple range test (OneWay ANOVA, P < 0.05) was used in SigmaPlot 12. For the assumptions of ANOVA we used Hartley's F_{max} test for homogeneity and the Shapiro-Wilk normality test.

3. Results

3.1. Zinc deficiency treatment causes reduced Zn and Fe content in the organs of Brassica

We first examined whether the reduction of the Zn content in the nutrient solution results in a reduced Zn content in the shoot and root of *Brassica napus* during the experimental period (Fig. 1 A). The Zn
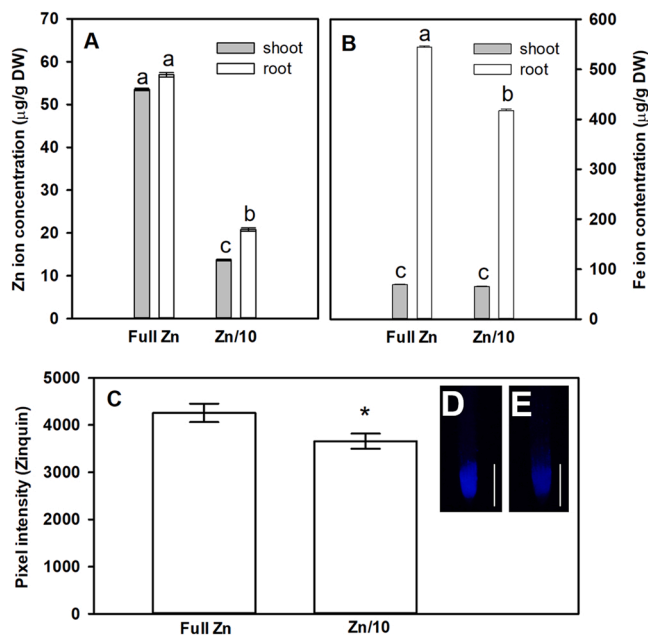
Fig. 1. Concentration of zinc (Zn, A) and iron (Fe, B) in shoots and roots of *Brassica napus* grown in the presence of optimal (full Zn, 5 μM $ZnSO_4$) or suboptimal (Zn/10, 0.5 μM $ZnSO_4$) Zn content for 21 days. Different letters indicate significant differences according to Duncan's test (n = 3, P ≤ 0.05) (C) Pixel intensities measured in Zinquin labelled root tips of *Brassica napus*. Significant differences are indicated by asterisks according to Student t-test (n = 10, *P ≤ 0.05). Representative microscope images taken of Zinquin-labelled root tips of *Brassica napus* grown in nutrient solution with optimal (D) or limited (E) Zn supply. Bars= 200 μm.

concentration was similar in both organs of plants grown in a nutrient solution with full Zn content, and it significantly decreased in case of Zn/10 treatment. In the shoot, the Zn content showed a ~75% decrease compared to the control, while in the root, this decrease proved to be ~64% (Fig. 1 A).

In contrast to Zn, the distribution of Fe within control plants was not homogeneous, and the root contained almost 8 times as much Fe as the shoot (Fig. 1 B). Zn limitation did not cause significant decrease in shoot Fe content. In contrast, Zn deprivation caused a significant diminution in root Fe content, although the rate of this (24%) was smaller than the decrease in Zn content.

Zn deficiency was detectable also at the tissue level in Brassica root tips, where Zn-related fluorescence in the apical meristem tissue showed reduced (by 15%) level in plants grown in Zn/10 solution (Fig. 1 CDE). The restriction of Zinquin-derived fluorescence to root meristem tissue can be explained by the fact that actively dividing meristematic cells with active metabolism require more Zn microelement than the surrounding tissues.

3.2. Brassica napus is sensitive to Zn deficiency

Based on the measured Zn concentrations and shoot biomass, the Zn deficiency tolerance index was calculated, which was compared for *Brassica napus* and *Pisum sativum* (tolerant species) (Table S2). *Pisum sativum* showed a tolerance index of around 100% when grown in the limited Zn-containing medium for three weeks, while the same growth condition caused a 46% decrease in the tolerance index of *Brassica napus*. The Zn efficiency value calculated from the Zn content of the shoot remained around 1 in the Zn-limited *P. sativum* and decreased to ~0.25 in *B. napus*. The suboptimal Zn concentration of the medium did not cause an increase in the Zn usage index compared to the control in *P. sativum*, but in *B. napus* the value increased two-fold due to the significant decrease of the shoot zinc content.

3.3. Limited Zn supply alters the levels and distribution of macro- and microelements in Brassica napus leaves

Using the LIBS technique, the distribution of Zn and other micro- and macroelements were mapped in *B. napus* leaves (Fig. 2). In general, macroelements, due to their higher tissue concentration, can be examined with higher efficiency than microelements using LIBS. However, there were elements in both groups of nutrients (e.g. copper, manganese, nickel) for which we could not obtain evaluable spectra. The distribution of the relatively weak signal of Zn was homogeneous in the leaf in case of adequate Zn supply, but it was restricted and accumulated slightly to the margins in the leaf of plants exposed to Zn deficiency treatment. Similar Zn deficiency-induced changes in distribution (accumulation at leaf margins) were observed also for molybdenum (Mo) and calcium (Ca). In case of Ca, a diminution of the total level in the leaf blade was also clearly detectable (Fig. 2).

For potassium (K), magnesium (Mg), and Fe, no Zn-deficiency triggered changes in distribution were detected, but we observed significantly reduced levels of these elements in the whole leaf blade.

Thus, in the case of successfully detected macronutrients, Zn deficiency resulted in their reduced content without any changes in spatial distribution. For Ca and the detected microelements, accumulation at leaf edges occurred due to Zn deficiency resulting in inhomogeneous distribution in the leaves.

3.4. Suboptimal Zn supply limits the biomass production and alters the root structure of B. napus

The fresh and dry weight of *B. napus* shoot were reduced by 44% and 46% due to Zn deprivation compared to optimal Zn, respectively (Fig. 3 AB). Fig. 3 D shows reduced shoot biomass of *B. napus*.

Cell viability measured in leaf discs was reduced by 40% due to Zn limitation, while there was no detectable viability loss in root tip cells (Fig. 3 C). However, the fresh and dry weight of Zn-deficient root was significantly reduced by 40% and 55%, respectively (Fig. 3 EF).

The decrease in root volume was indicated also by the fact that the plants growing with suboptimal Zn supply suffered a 25% primary root shortening (Fig. 3 G) and the number of their lateral roots was halved compared to control (Fig. 3 H).

3.5. Zn deficiency induces changes in the levels of sugars and sugar derivatives in Brassica napus

Metabolomics analysis revealed a complex response to Zn deficiency. Zn limitations did not cause statistically significant changes in the investigated amino acids (Ser, Thr, Val, Gly) contents, and others (Ala, Leu, Ile, Phe, Asn, and Tyr) were under the detection limit (data not shown). In contrast, the concentration of certain sugars and sugar phosphates namely glucose, D-fructose 6-phosphate, glucose 6-phosphate, and mannose 6-phosphate but not fructose significantly decreased in the root samples as the effect of Zn limitation (Table S3).

3.6. Zn deficiency disturbs ROS metabolism and induces redox imbalance in Brassica napus

The blue colorization during the histochemical detection of $O_2^{\bullet-}$ indicated that Zn-deficient leaves contained elevated levels of this ROS compared to leaves derived from the adequately supplied plants (Fig. 4 A). In contrast, H_2O_2 levels labelled by DAB staining did not differ in control and Zn-deficient Brassica leaves (Fig. 4 A).

The $O_2^{\bullet-}$ level in the root apex was detected using fluorescent probe, and it was found that the related fluorescence did not change significantly due to Zn limitation (Fig. 4 B), in contrast to H_2O_2, which showed approx. two-fold accumulation in Zn-deficient roots (Fig. 4 CD).

Regarding the levels of both ROS, shoot and root showed opposite changes, as $O_2^{\bullet-}$ levels increased in the leaf and did not change in the root,
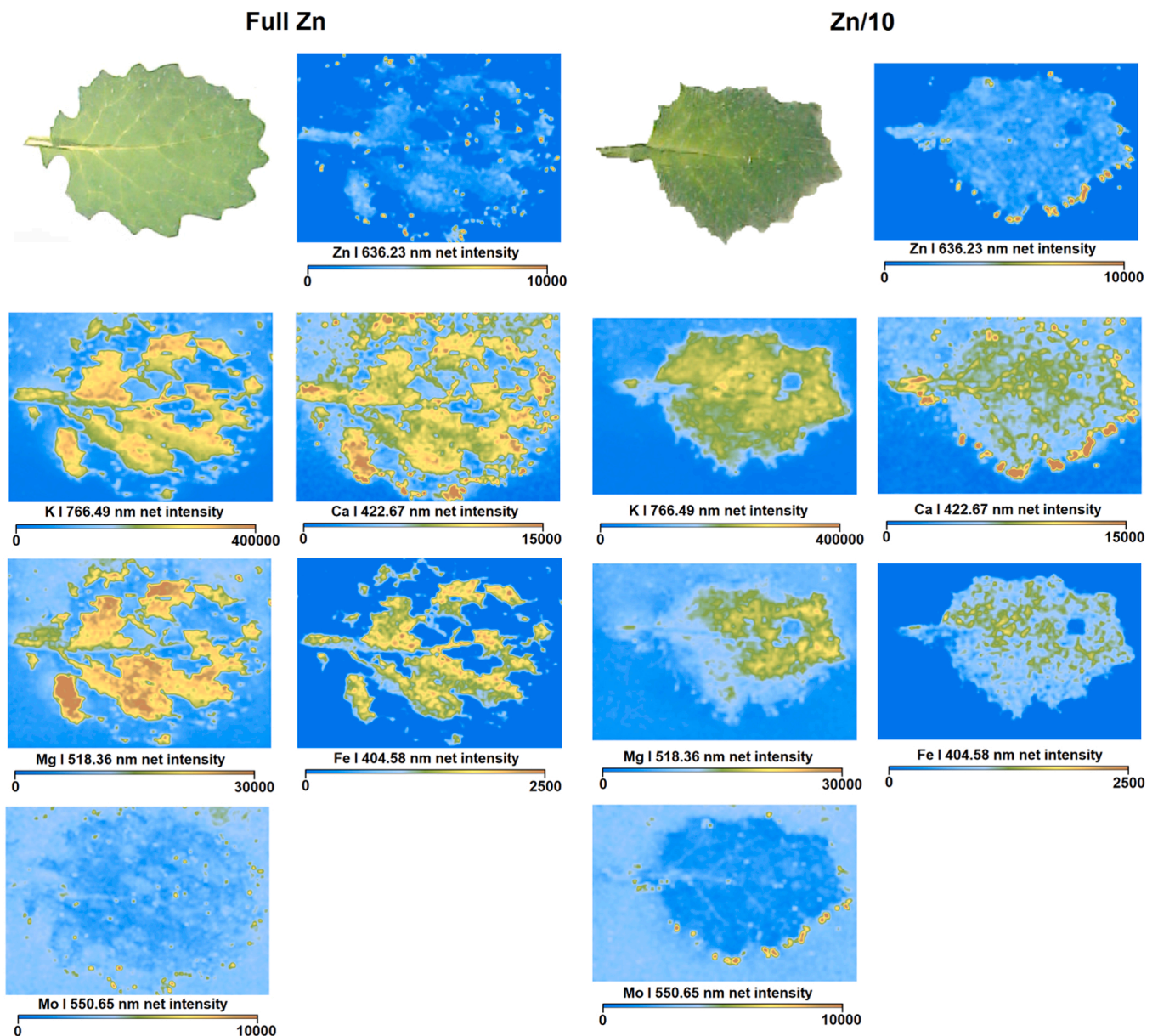
Full Zn   Zn/10

Fig. 2. Optical microscopy image and LIBS elemental distribution maps of leaves derived from *Brassica napus* plants grown in nutrient solution with optimal (Full Zn, 5 μM ZnSO₄) or suboptimal (Zn/10, 0.5 μM ZnSO₄) Zn supply for 21 days. The colour of the scale, from blue to brown, is indicating increasing signal intensities.

while H_2O_2 did not accumulate in the leaves, but its levels almost doubled in Zn-deficient root tips. Therefore, we examined the activity of NOX isoenzymes responsible for $O_2^{\bullet-}$ production and identified 3 isoenzymes in the shoot and two isoenzymes in the root with weaker activities (Fig. 4 E, Fig. S1). Zn deficiency induced the activity of all identified NOX isoenzymes. The total activity of the superoxide anion-eliminating SOD enzymes was halved in the Zn limited shoot, while the decrease in SOD activity in Zn-deficient roots was ~30% compared to plants adequately supplied with Zn (Fig. 4 F). One MnSOD, two FeSODs and three Cu/Zn SODs were identified in roots, while one FeSOD and three Cu/Zn SODs showed activity in *Brassica napus* shoot (Fig. 4 G, Fig. S2). The activity of shoot SOD isoenzymes decreased, but the FeSOD activity in the root increased significantly together with the decrease of other SOD isoenzymes in Zn-deficient plants compared to the control (Fig. 4 G, Fig. S2). This may have contributed to the mitigation of Zn deficiency-induced $O_2^{\bullet-}$ production in the root.

Among the APX isoenzymes involved in H_2O_2 detoxification, thylakoid APX (tAPX) was identified in *Brassica napus* shoot and two

cytoplasmic isoenzymes in root and shoot, of which root cAPX enzymes are present in higher amounts (Fig. 5 A, Fig. S3). In Brassica shoot, the amount of all three isoenzymes decreased (tAPX by ~30%, cAPX1 by ~10%, cAPX2 by 15%) while in the root, the abundance of both detected isoenzymes increased (cAPX1 by 8%, cAPX2 by 17%) due to Zn deprivation (Fig. 5 A, Fig. S3). The concentration of AsA_red in the adequately Zn-supplied Brassica shoot exceeded that of the root, while the amount of AsA_ox was found to be similar in both organs (Fig. 5 B). Zinc deprivation resulted in a 45% decrease in AsA_red concentration in both the shoot and the root (Fig. 5 B) and the amount of AsA_ox in root and shoot of Zn-deprived Brassica was unchanged (Fig. 5 B). In contrast to ascorbate, changes in glutathione quantities showed organ dependence (Fig. 5 C). In the Zn-deficient Brassica shoot, the concentration of GSH_red decreased by ~50%, while in the root it increased by 60% compared to the control. The amount of GSH_ox showed Zn deficiency-induced changes neither in the shoot no in the root system. In the root of Zn-deficient plants, the amount of GSH_red+ox significantly exceeded that of the Zn-deficient shoot, and the GSH_red:GSH_ox ratio shifted in none
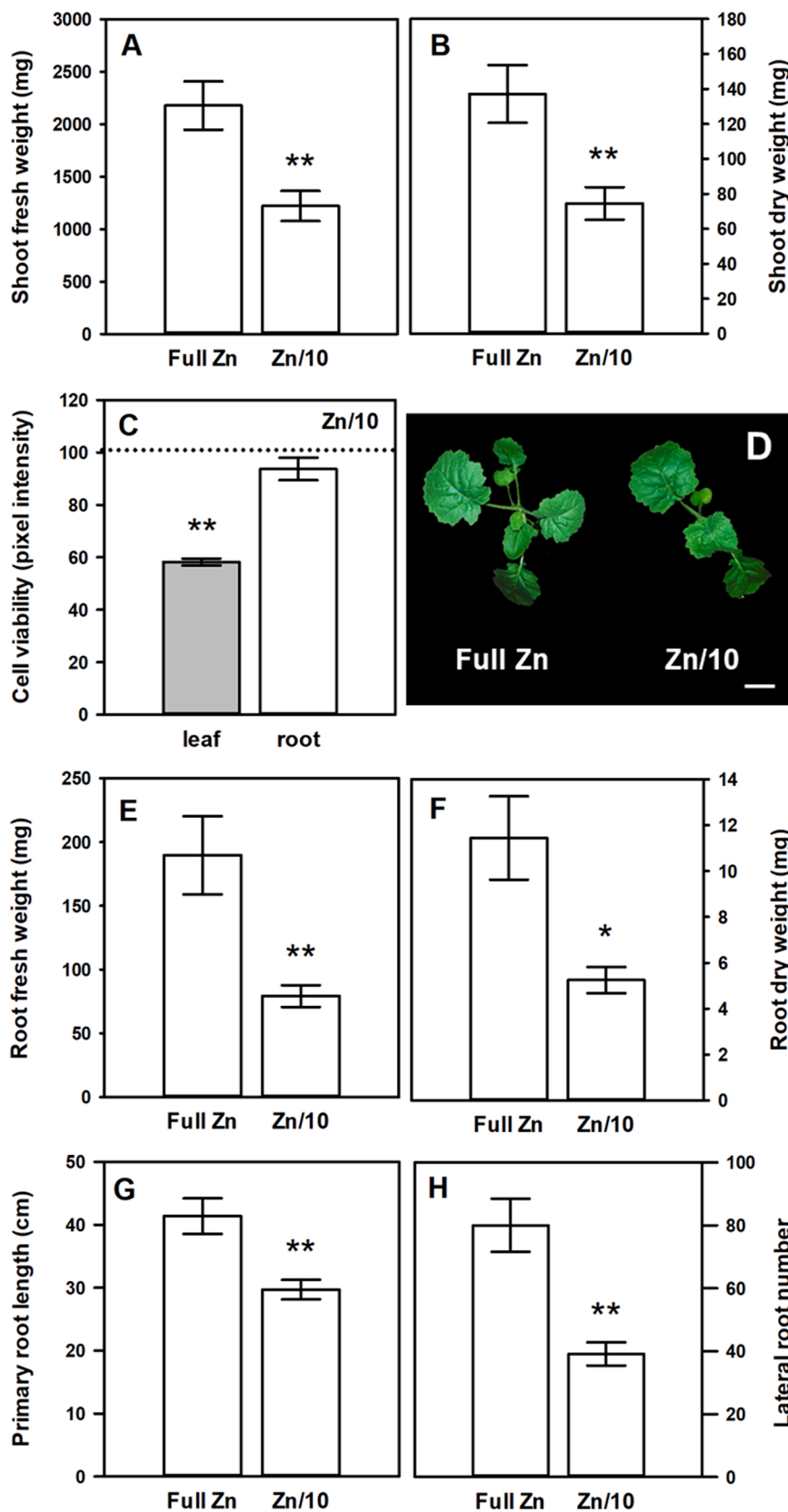
Fig. 3. Shoot fresh (A) and dry weight (B) of *Brassica napus* grown in a nutrient solution with optimal (full Zn, 5 μM ZnSO$_4$) or suboptimal (Zn/10, 0.5 μM ZnSO$_4$) Zn content for 21 days. (C) Cell viability in the root apical meristem of Zn-limited *Brassica napus* expressed as pixel intensity of fluorescein. Dashed line indicates 100% cell viability for the control (Full Zn) plants. (D) Photographs taken from the shoot of *Brassica napus* grown in the presence of optimal and suboptimal Zn supply. Bar= 2 cm. Root fresh (E), dry weight (F), primary root length (G) and lateral root number (H) of *Brassica napus*. Significant differences are indicated by asterisks according to Student *t*-test (n = 10–60, *P ≤ 0.05, **P ≤ 0.01).

of the organs.

3.7. Zn deficiency disturbs RNS metabolism in sensitive Brassica napus

The most common RNS (NO, ONOO⁻, GSNO) were detected by fluorescent probes in Brassica leaves and roots. Interestingly, the level of
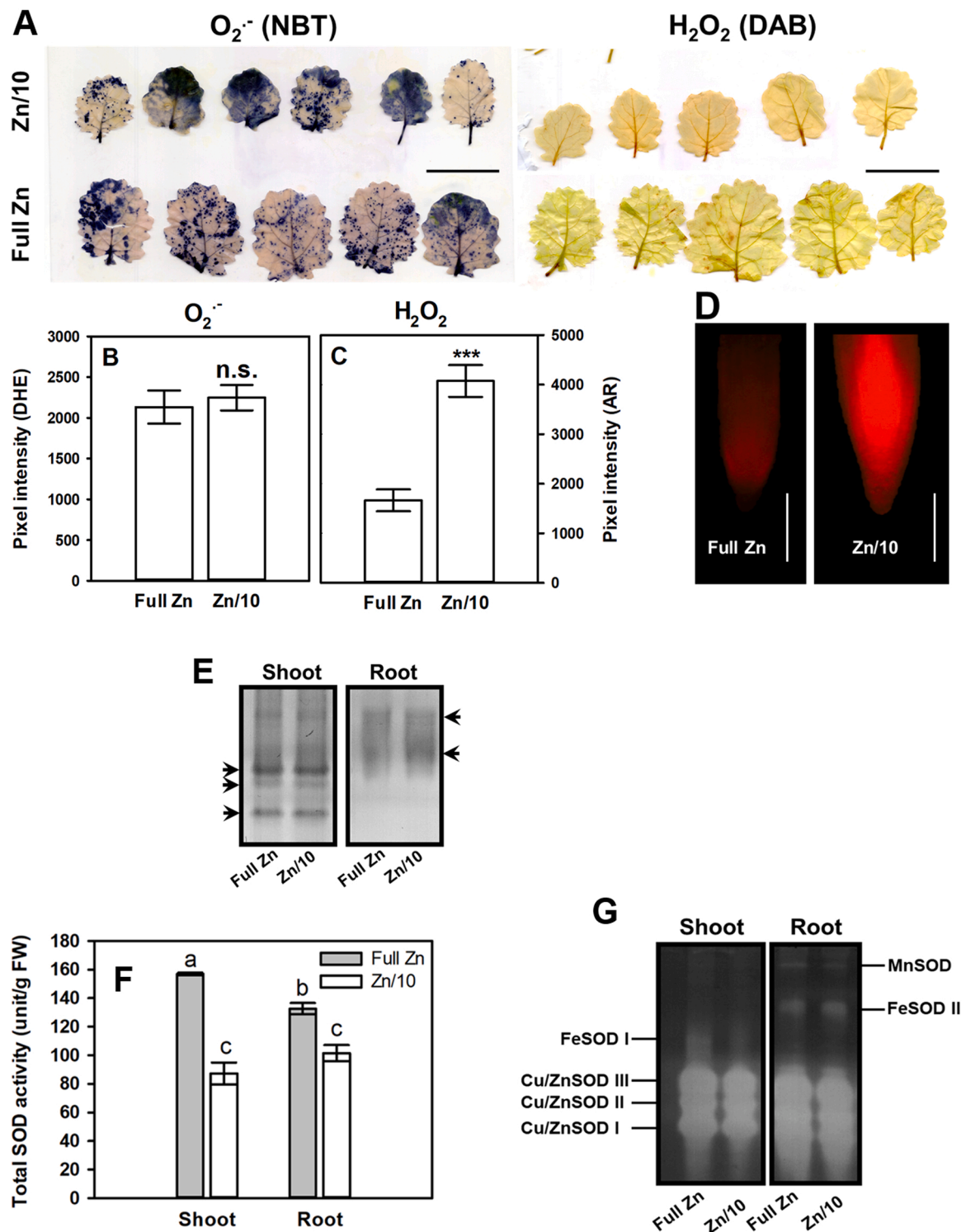
Fig. 4. Histochemical detection of superoxide anion ($O_2^{•-}$) using nitroblue tetrazolium (NBT, A) and hydrogen peroxide (H_2O_2) using 3–3-diaminobenzidine (DAB, A) in the leaves of *Brassica napus* grown in nutrient solution with optimal (full Zn, 5 μM $ZnSO_4$) or suboptimal (Zn/10, 0.5 μM $ZnSO_4$) Zn content for 21 days. Bars= 3 cm. $O_2^{•-}$ (B) or H_2O_2 (C) levels in the root tips expressed as pixel intensities of fluorescent probes. Significant differences are indicated by asterisks according to Student t-test (n = 10, ***P ≤ 0.001, n.s.=non-significant). (D) Representative microscopic images taken from Amplex Red-labelled roots tips of *Brassica napus* indicating H_2O_2 levels. Bars= 200 μm. (E) Native PAGE separation of NADPH oxidase (NOX) isoenzymes in the shoot and root of *Brassica napus*. Putative NOX isoenzymes are indicated by asterisks. (F) Total SOD activity in the shoot and root of *Brassica napus*. Different letters indicate significant differences according to Duncan's test (n = 5, P ≤ 0.05). (G) Native PAGE separation of superoxide dismutase (SOD) isoenzymes in the shoot and root of *Brassica napus* grown in full or Zn deficient nutrient solution.
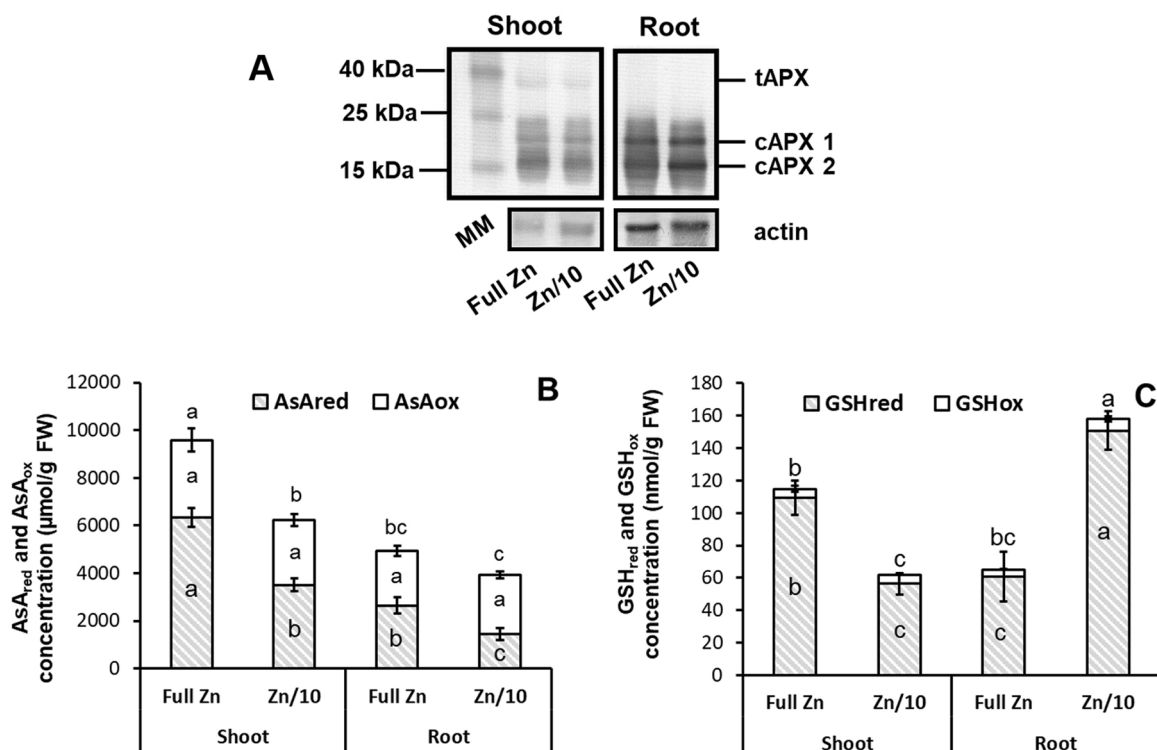
Fig. 5. (A) Representative immunoblot probed with anti-APX from protein extracts of *Brassica napus* shoot and root. Plants were grown in nutrient solution with optimal (full Zn, 5 μM ZnSO$_4$) or suboptimal (Zn/10, 0.5 μM ZnSO$_4$) Zn content for 21 days. Tylakoid (tAPX) and cytoplasmic (cAPX1 and cAPX2) APX isoforms were identified. Western blot with anti-actin is shown as loading control. Concentrations of reduced (AsA$_{red}$) and oxidized (AsA$_{ox}$) ascorbate (μmol/g FW, B) and reduced (GSH$_{red}$) and oxidized (GSH$_{ox}$) glutathione (μmol/g FW, C) in shoots and roots of *Brassica napus*. Different letters indicate significant differences according to Duncan's test (n = 5, p ≤ 0.05).

NO in both organs was elevated by Zn deprivation, and the rate of NO accumulation was lower in the leaves (~10%) than in the root (200%) (Fig. 6 AB). The level of ONOO⁻ formed in the reaction between NO and O$_2^{\bullet-}$ showed an increase with similar extent (~10% in leaf, ~15% in root) in both *Brassica napus* organs due to Zn limitation (Fig. 6 CD). As for the amount of GSNO, an increase of ~10% in the leaves and a decrease of 64% in the roots was observed due to Zn limitation (Fig. 6 EF).

The expression of *NIA1* was reduced (by 50%) in the shoot but induced (by two-fold) in the root by Zn deficiency (Fig. 7 A). The expression of *GLB1* showed two-fold induction as the effect of limited Zn supply in Brassica roots, but not in the shoot system (Fig. 7 C). Regarding *GLB2*, its expression showed Zn deficiency-induced decrease (by 38%) in the root, and was unmodified in the shoot compared to adequate Zn supply (Fig. 7 D).

The *GSNOR1* showed decreased (by 28%) expression in the shoot due to Zn deprivation; however, a 2-fold induction was observed in the root of Zn-deficient plants compared to control (Fig. 7 B). Reduced Zn availability resulted in a 20% diminution of GSNOR abundance in the shoot system, and a 12% reduction in the root system compared to plants with optimal Zn supply (Fig. 7 E). Furthermore, GSNOR activity was slightly (by 20%) decreased in the shoot and was not significantly changed in the root by insufficient Zn supply (Fig. 7 F).

3.8. Zn deficiency triggers changes in the nitro-oxidative status

Protein tyrosine nitration, a reliable marker of nitrosative stress, was detected by western blot analysis in whole root and shoot extracts of *Brassica napus* (Fig. 8 A).

Protein bands affected by tyrosine nitration were observed in both organs of healthy *Brassica napus* adequately supplied with Zn. In the shoot, Zn deficiency enhanced the immune positive response of anti-3-nitrotyrosine antibody in one protein band (indicated by black arrow

in Fig. 8 A) and decreased it in at least 3 additional bands (indicated by grey arrows in Fig. 8 A). A single protein band was detected in which 3-nitrotyrosine appeared only in the Zn deficient condition (indicated with white arrow in Fig. 8 A). As the effect of Zn limitation, no protein band containing new nitrated proteins in the root appeared on the membrane, but the nitration signal was enhanced for at least 8 low molecular weight protein bands (indicated by black arrows in Fig. 8 A).

Protein carbonylation due to ROS accumulation was also detected in the organs of *Brassica napus*. In the shoot of Zn-deprived plants, protein carbonylation was intensified compared to control in at least 6 protein bands (indicated by black arrows in Fig. 8 B). Moreover, two immune positive band with higher molecular weight appeared on the membrane due to Zn limitation (indicated by white arrows in Fig. 8 B).

4. Discussion

4.1. Zinc deficiency treatment causes reduced Zn and Fe content in the organs of Brassica

For most plant species, a decrease in the shoot Zn content below 15–20 μg/g DW indicates Zn deficiency (Marschner, 2012; Noulas et al., 2018). The measured Zn concentration (13.7 μg/g DW, Fig. 1 A) in the shoot system of *Brassica napus* reflects that the reduction in the Zn content of the nutrient solution resulted in Zn deficiency during the 21-day treatment period.

It has been repeatedly supported by experimental data that Fe deficiency leads to Zn accumulation, while surplus Zn causes Fe deficiency symptoms (Haydon et al., 2012; Shanmugam et al., 2012; Briat et al., 2015). However, much less is known about the effect of Zn deprivation on tissue Fe concentrations and also the molecular explanations are missing. Similar to our results, Saenchai et al. (2016) observed control-like Fe content in the shoot and reduced Fe content in the root of
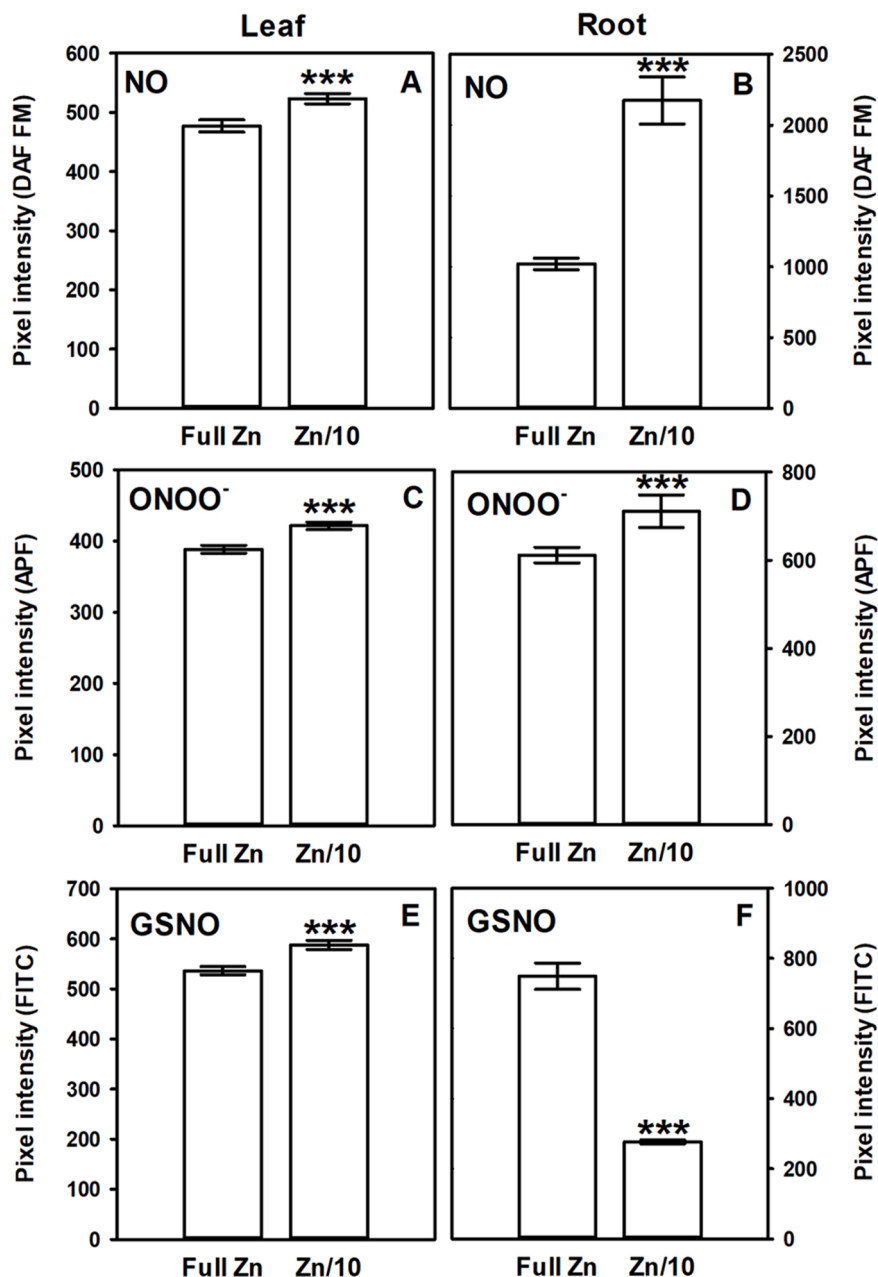
Fig. 6. Nitric oxide (NO, AB), peroxynitrite (ONOO-, CD) and *S*-nitrosoglutathione (GSNO, EF) levels in leaves and root tips of *Brassica napus* grown in nutrient solution with optimal (full Zn, 5 μM ZnSO$_4$) or suboptimal (Zn/10, 0.5 μM ZnSO$_4$) Zn content for 21 days. Significant differences are indicated by asterisks according to Student *t*-test (n = 10, ***P ≤ 0.001).

Zn-deprived wild type rice. Diminution in root Fe level triggered by suboptimal Zn concentration (Fig. 1 B) suggests that there is an interaction between the uptake of Zn and Fe in the root system, and decreased Zn uptake may also limit the absorption of Fe.

4.2. Brassica napus is sensitive to Zn deficiency

Zinc deficiency tolerance indexes, Zn efficiency and Zn usage indexes were calculated and compared for *B. napus* and *P. sativum* grown in full and Zn-limited nutrient solutions in order to evaluate the relative sensitivity of *B. napus* to Zn limitation (Table S2). These indicators together with the tissue Zn concentration data (Fig. 1 AC) highlight that *Brassica napus* (cv. Negro Caballo) is sensitive to Zn deficiency, since highly reduced shoot Zn levels were caused by a short-term, mild Zn deprivation during laboratory conditions. *Pisum sativum* is known to be

tolerant to inadequate Zn supply (Alloway, 2008), which is supported by our comparative experiment. Although, this work didn't aim to examine Zn deficiency responses at the genotype-level, it has to be noted that slight differences can be observed in Zn efficiency of different canola and pea genotypes (Grewal et al., 1997; Grewal and Graham, 1997; Pandey et al., 2012).

4.3. Limited Zn supply alters the levels and distribution of macro- and microelements in Brassica napus leaves

Our results support that LIBS allows the non-destructive spatial visualization of metal abundance in intact leaves and can detect multiple elements simultaneously with a low detection limit (0.01 μg/g) (McRae et al., 2009; Wu et al., 2009a,b; Callahan et al., 2016; Huang et al., 2018). Beyond these, we evidenced that both reduced Zn levels and
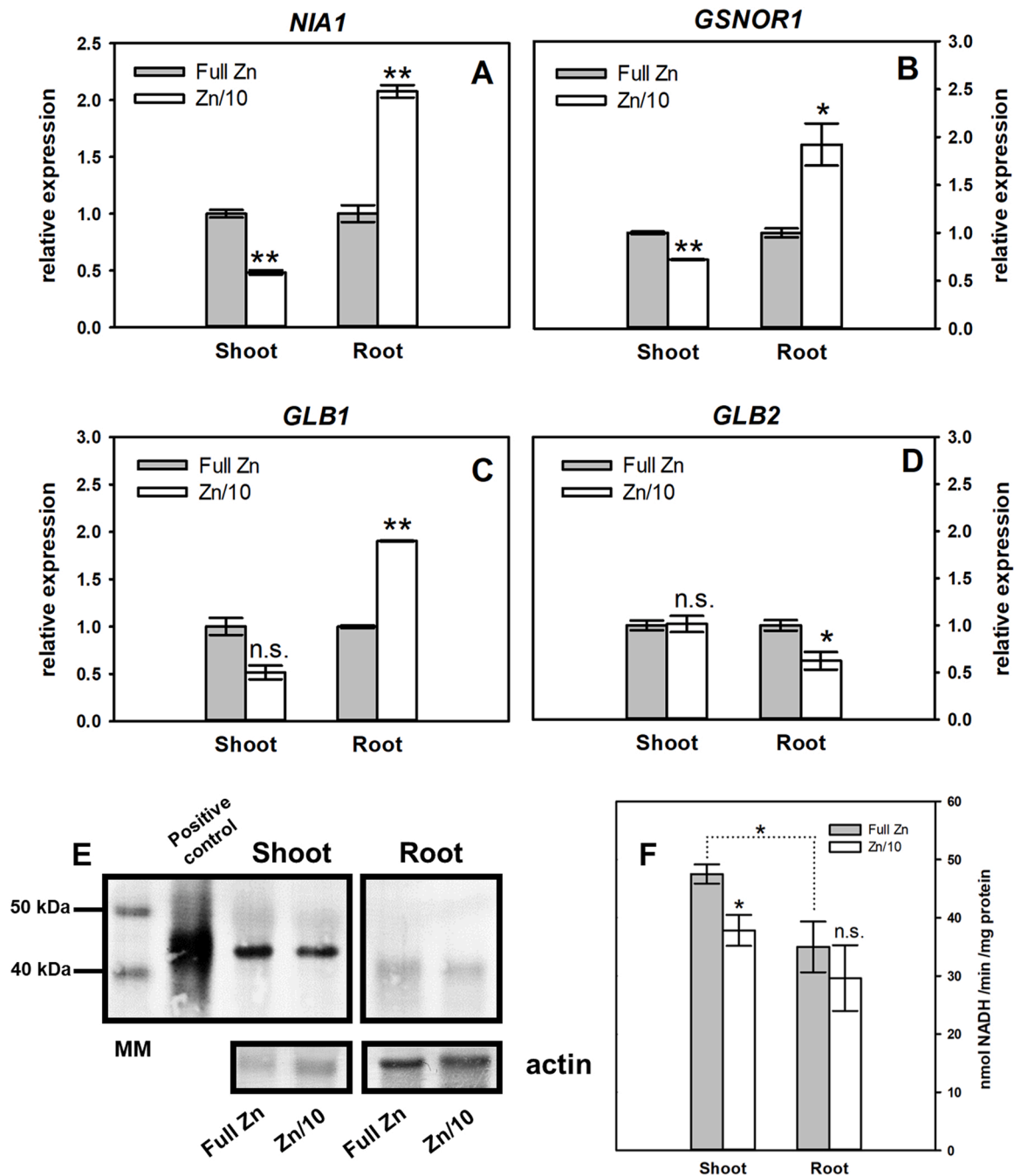
Fig. 7. (A-D) Relative transcript level of selected NO-associated genes (*NIA1, GSNOR1, GLB1, GLB2*) in the shoot and root of *Brassica napus* grown in full (Full Zn, 5 μM $ZnSO_4$) or Zn-limited (Zn/10, 0.5 μM $ZnSO_4$) nutrient solutions for 21 days. Data were normalized using the *B. napus ACTIN7* gene as internal controls. The relative transcript level in control samples was arbitrarily considered to be 1 for each gene. (E) Western blot probed with anti-GSNOR antibody. Western blot with anti-actin is shown as loading control. Protein extract from GSNOR overproducer *35 S::FLAG-GSNOR1 Arabidopsis thaliana* was used as positive control. (F) GSNOR activity (nmol NADH/min/mg protein) in the shoot and root system of control and Zn-deprived *Brassica napus*. Significant differences are indicated by asterisks according to Student *t*-test (n = 5, *P ≤ 0.05, **P ≤ 0.01, ***P ≤ 0.001, n.s.=non-significant).

altered elemental distribution can be visualized in leaves of Zn-deficient plants by using LIBS which raises the possibility that this technique can be applied for the fast and non-invasive monitoring of Zn-deficient plants.

According to the results of our LIBS analyses, the Zn-limited plants concentrate some of the elements like Zn, Mo and Ca in leaf margins, which are regions of actively growing cells. Here, the accumulation of the elements may inhibit growth and induce visible symptoms like necrosis (see Fig. 2). Based on the analyses, it can be stated that the homeostasis of macro- and microelements is disturbed, with changes in the

tissue distribution of some elements in the leaves of *B. napus* growing with inadequate Zn supply.

4.4. Suboptimal Zn supply limits the biomass production and alters the root structure of B. napus

Suboptimal Zn supply caused notable retardation of Brassica shoot growth and development which is indicated by the substantial reduction in both the fresh and the dry weight of the shoot system (Fig. 3 AB). The decrease of cell viability in the leaf indicates extended cell death which
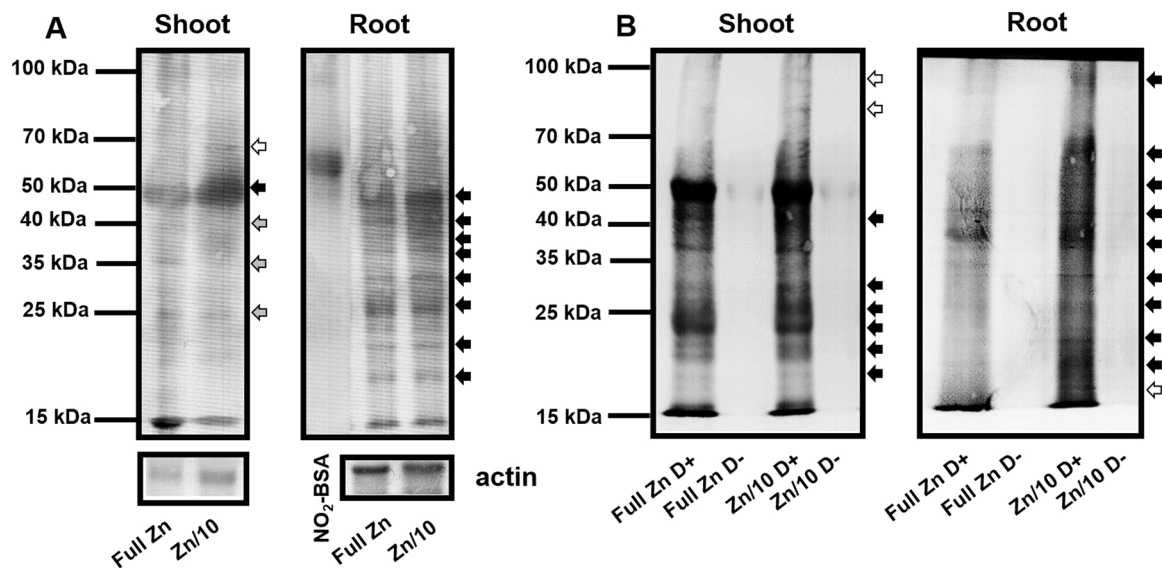
Fig. 8. Protein tyrosine nitration and protein carbonylation in shoot and root *of Brassica napus* grown in full (Full Zn, 5 μM ZnSO₄) or Zn-limited (Zn/10, 0.5 μM ZnSO₄) nutrient solutions for 21 days. Representative immunoblot probed with an antibody against 3-nitro-tyrosine showing nitrated proteins (A) and immunoblot probed with anti-DNP antibody presenting carbonylated proteins (B). Western blot with anti-actin is shown as loading control. Commercial nitrated BSA (NO₂-BSA) was used as a positive control of protein nitration. Samples without derivatization (D-) are shown as controls for protein carbonylation. White arrows indicate protein bands being present only in Zn-limited plants. Black arrows indicate protein bands in which nitration/carbonylation increased as the effect of Zn limitation. Grey arrows indicate protein bands in which nitration decreased as the effect of suboptimal Zn supply.

may be the cellular-level reason for malfunction and decreased biomass production. Based on the more detailed examination of the root system, it can be suggested that the decrease in primary root elongation together with inhibited lateral root development contributes to the Zn limitation-induced decrease of fresh and dry weight. Despite the suboptimal Zn-induced primary root shortening, there was no detectable decrease in meristem cell viability. This suggests that a disturbance in phytohormone homeostasis as the effect of Zn limitation may cause the retardation in the root growth.

The major phytohormone that controls root growth is IAA, which is produced from tryptophan as a precursor in Brassicaceae (Mano and Nemoto, 2012). Zinc directly activates tryptophan synthase (Horák et al., 1976), and reduced IAA levels in Zn-deficient plants have been observed by several authors (Horák et al., 1976; Cakmak et al., 1989; Alloway, 2008; Wang et al., 2021). Based on these it is hypothesized that the synthesis of the amino acid as well as the phytohormone may be insufficient leading to the inhibition of root growth during Zn deficiency. Furthermore, the retardation of shoot and root biomass production as the effect of short-term mild Zn deprivation reflects the sensitivity of *B. napus* to Zn deficiency.

4.5. Zn deficiency induces changes in metabolites like sugars and sugar derivatives in Brassica napus

Based both on literature data and our experimental root and shoot growth data, we suggested that there may be Zn limitation-triggered differences in sugar metabolism of *Brassica napus*. Therefore, a metabolomics study was performed during which not only amino acids, but also sugars and sugar derivatives were detected in the shoot and root of control and Zn-deficient *B. napus*. Compared to control samples, decrease could be observed in case of fructose, glucose, D-fructose 6-phosphate, glucose 6-phosphate and mannose 6-phosphate (Table S3). These data suggest a disturbed cell metabolism as the effect of inadequate Zn supply, which could contribute to growth reduction. The more significant reduction of sugar levels in the root indicates that translocation of produced sugars to roots could be insufficient affecting root growth.

4.6. Zn deficiency disturbs ROS metabolism and induces redox imbalance in Brassica napus

First of all, it should be noted, that in cases of both NBT and DAB staining, the leaves of plants with suboptimal Zn supply appear to have smaller size compared to the leaves of plants grown in complete nutrient solution, suggesting that Zn deficiency may restrict leaf expansion, which may contribute to the observed retardation in shoot biomass production (Fig. 3 ABD).

Zinc limitation caused $O_2^{\bullet-}$ and H_2O_2 production in *Brassica napus* similar to other plant species like bean, tomato, cotton (Cakmak and Marschner, 1988) but these effects were dependent on the organ of the plant (Fig. 4 A-D). Therefore, the enzymatic system controlling ROS levels was also examined. In our experiments, the activation of NOX isoenzymes (Fig. 4 E) together with the uniform decrease in SOD activities in the shoot (Fig. 4 F) may explain the increase in $O_2^{\bullet-}$ levels induced by Zn deficiency. Our results not only support the previous observations that suboptimal Zn supply in plants results in elevated ROS levels partly due to the activation of NOX (Cakmak and Marschner, 1988; Pinton et al., 1994; Cakmak, 2000) but also provide the first evidence for Zn deficiency-induced NOX isoenzymes in *B. napus* (Fig. 4 E). Beyond NOX activation, suboptimal Zn-triggered ROS generation involves also the down-regulation of the activities of antioxidant enzymes (SOD, POX, APX, GR) (Cakmak, 2000; Sharma et al., 2004; Wang and Jin, 2007; Tewari et al., 2019; Shinozaki et al., 2020).

The changes in APX abundance (Fig. 5 A) suggest that APX-dependent detoxification may be activated in the root and inactivated in the shoot as the effect of Zn limitation, although these changes do not show a direct correlation with H_2O_2 levels (Fig. 4 B and D) in these organs. In previous works, the activity of APX was shown to be decreased by inadequate Zn supply in wheat and pea (Sharma et al., 2004; Pandey et al., 2012), while low Zn stress resulted in increased APX activity in rice roots (Rose et al., 2012) supporting our results.

The significant decrease in AsA_red concentration as the effect of Zn deprivation in both the shoot and the root (Fig. 5 B) supports the results of Höller et al. (2014) who demonstrated that the redox imbalance under Zn deficiency is partly due to inhibited ascorbate biosynthesis. This is further corroborated by the unchanged amount of AsA_ox in root and

shoot of Zn-deprived Brassica (Fig. 5 B), indicating that no $AsA_{red} \rightarrow AsA_{ox}$ conversion occurred, but the synthesis of the AsA_{red} form may have decreased due to suboptimal Zn supply. The AsA_{red}:AsA_{ox} ratio shifted due to the predominance of the AsA_{ox} form as the consequence of the Zn deficiency-triggered decrease in the content of AsA_{red}. Our results support the hypothesis of Höller et al. (2014) that ascorbate plays an important role in maintaining cellular redox homeostasis and avoiding oxidative stress under Zn deficiency. Also the glutathione levels of *Brassica napus* plants responded to Zn limited condition and the induced changes proved to be organ-dependent (Fig. 5 C). Moreover, the GSH_{red}:GSH_{ox} ratio shifted in none of the organs. However, these observations contradict those of Tewari et al. (2019) who demonstrated that Zn limitation doesn't influence ascorbate or glutathione levels in the relatively sensitive maize cultivar, while increases both ascorbate and glutathione contents in the leaves of the relatively tolerant maize cultivar. Based on our results, suboptimal Zn supply does not seem to cause shifts in the oxidation state of ascorbate and glutathione but influences the amounts of the reduced forms in *Brassica napus* consequently leading to redox imbalance.

4.7. Zn deficiency disturbs RNS metabolism in sensitive Brassica napus

Brassica plants responded to Zn deprivation with elevated levels of NO and $ONOO^-$ in both of their organs (Fig. 6 A-D). The levels of GSNO were also affected by low tissue Zn content, but the changes were different in the organs (Fig. 6 EF). The notable Zn limitation-induced diminution of GSNO levels in the roots means that less GSNO may be formed, resulting in elevated levels of NO and GSH precursors compared to control. According to our knowledge, this is the first report to demonstrate the changes in endogenous RNS levels as the effect of limited Zn supply and the data suggest that the levels of the examined RNS molecules are highly responsive to Zn deprivation in *Brassica napus*.

Nitrate reductase (NR) involved in both nitrogen assimilation and NO synthesis is encoded by *NIA1* gene in *Brassica napus* (He et al., 2021). The Zn deficiency-induced reduction of *NIA1* gene expression (Fig. 7 A) indicates the involvement of N metabolism in Zn deficiency responses. Zn regulates N metabolism as a catalytic and structural constituent of enzymes (Broadley et al., 2007). Moreover, the contribution of Zn to N metabolism is supported by its positive effect on N use efficiency (Das and Green, 2013). In previous works, Zn deficiency led to reduced (Seethambaram and Das, 1986) or unchanged NR activity (Paradisone et al., 2021). Here, NR was examined at the transcript level and organ-specific response in *NIA1* gene expression was observed as the effect of mild Zn deficiency. Although, NR can be an enzymatic source of endogenous NO production, Zn deficiency-induced changes in *NIA1* gene expression can only be partially associated with NO production. Increased expression of *NIA1* in the root may contribute to Zn deficiency-induced NO production (Fig. 6 B), but a decrease in the expression in the shoot is not associated with the slightly increased NO levels (Fig. 6 A). The products of the *GLB1* and *GLB2* phytoglobin genes are involved in, among other things, NO elimination (Stasolla et al., 2019). Our results demonstrate that the Zn deficiency-induced elevation in *GLB1* expression in Brassica roots does not lead to decreased NO levels, whereas a decrease in *GLB2* expression may contribute to high NO levels in Zn-deprived plants (Fig. 7 CD).

The GSNOR enzyme was studied at multiple levels because it requires Zn cofactor and it catalyses the degradation of GSNO, thus it is a master regulator of NO signaling. GSNOR from *Brassica oleraceae* was characterized by Tichá et al. (2017a). In the shoot, both gene expression (Fig. 7 B) and protein production (Fig. 7 E) decreased slightly as a prelude to the slightly decreased activity, meaning that the regulation of GSNOR by Zn deficiency in this organ occurs at the transcriptional level. In contrast, a decrease in protein abundance in the root, in addition to an increase in *GSNOR1* expression, suggest that Zn deficiency regulates the enzyme at the (post)translational level. However, the Zn deficiency-induced decrease in protein amount doesn't result in

significantly reduced enzyme activity. The posttranslational regulation of GSNOR can be realized through different ways. Hydrogen peroxide produced as a result of Zn deficiency may cause oxidative modifications on Cys47 and Cys177 coordinating Zn^{2+} cofactor consequently leading to Zn ion release and reduced activity of GSNOR (Kovács et al., 2016). Interestingly, GSNOR is susceptible for *S*-nitrosation on non-zinc-chelating Cys residues (Cys10, Cys271 and Cys370) and the slight structural modification leads to reduced specific activity (Guerra et al., 2016; Tichá et al., 2017b; Lindermayr, 2018). Another possible way of suboptimal Zn-triggered inactivation of GSNOR may be due to the limited amount available of Zn^{2+} cofactor which can be considered as a ROS/RNS-independent and Zn supply specific regulatory effect on GSNOR. The inhibition of GSNOR results in elevated SNO levels and intensified NO signalling (Lindermayr, 2018). According to Kolbert et al. (2019) excess Zn-induced H_2O_2 directly decreases GSNOR activity which leads to the *S*-nitrosation of certain antioxidant enzymes (APX, CAT) in Arabidopsis. In case of inadequate Zn supply, a similar regulatory mechanism is conceivable.

4.8. Zn deficiency triggers changes in the nitro-oxidative status

Protein tyrosine nitration is a marker of nitrosative stress therefore it was examined in the organs of *B. napus* (Fig. 8 A). Due to Zn limitation-induced tyrosine nitration of some protein bands, and intensification, or decrease in nitration of other protein bands it can be suggested that the protein nitration pattern is changed in the shoot of plants exposed to Zn deficiency compared to the shoot of healthy plants. In the Zn-deficient Brassica root, the results suggest an increase in protein tyrosine nitration. Collectively, it is observed for the first time that inadequate supply of a micronutrient intensifies nitrosative modification of plant proteins. Increased levels of nitrated proteins have been described in different plant species subjected to diverse abiotic stresses like water deprivation, high or low temperature, excess Zn or nickel supply etc. (Signorelli et al., 2013; Chaki et al., 2013; Airaki et al., 2012; Feigl et al., 2015, 2020; reviewed in Corpas et al., 2021).

Beyond tyrosine nitration, protein carbonylation due to ROS accumulation plays a role in proteome remodelling under stress conditions. In *Brassica napus*, suboptimal Zn supply resulted in increased carbonylation of shoot and root proteins (Fig. 8 B) similar to the results of Shinozaki et al. (2020) who observed higher level of protein carbonylation induced by Zn deficiency in Arabidopsis autophagia mutant *NahG atg5* than in the wild type. These results highlight also that autophagy is involved in moderating protein carbonylation induced by suboptimal Zn supply (Shinozaki et al., 2020).

The Zn-deficiency induced intensification of nitrosative (Fig. 8 A) and oxidative (Fig. 8 B) protein modifications indicate that proteins in both organs are more affected by carbonylation than nitration. Both nitrosative and oxidative protein modifications lead to the proteasomal degradation of the modified proteins (Tanou et al., 2012; Castillo et al., 2015; Ciacka et al., 2020) thus representing key cellular processes that help recycle amino acids during stress conditions. The role of 26 S proteasomes in Zn deficiency stress was demonstrated by the greater accumulation of polyubiquitinated proteins in *rpt2a* and *rpt5a* mutants than in wild type during Zn deficiency treatment (Sakamoto et al., 2011).

5. Conclusions

Reducing the Zn concentration in the nutrient solution leads to the development of *Brassica napus* plants with decreased tissue Zn, Fe contents and stunted shoot and root growth. Based on calculated parameters (Zn deficiency tolerance index, Zn efficiency and Zn usage index) *B. napus* proved to be relatively sensitive to Zn limitation compared to the tolerant *Pisum sativum*. Zn deficiency is accompanied by disturbed nutrient homeostasis in the leaves. Moreover, the reduced contents of sugars and sugar phosphates indicate disturbance in carbon metabolism

in Zn limited *Brassica napus*. Zinc deficiency-induced secondary oxidative stress was evidenced by the imbalance in ROS ($O_2^{\bullet-}$, H_2O_2) homeostasis due to disturbed antioxidant defence. Furthermore, we first evidenced that Zn limitation triggers the overproduction of RNS (NO, $ONOO^-$, GSNO) in the shoot and root system of *Brassica napus* and due to ROS and RNS imbalance protein carbonylation and nitration occurs leading to nitro-oxidative stress. Collectively, Zn deficiency affects several physiological processes such as nutrient homeostasis, carbon, ROS and RNS metabolism in sensitive crop species *Brassica napus*.

Funding

CRediT authorship contribution statement

MÁ, Investigation, Methodology, Writing – original draft; **SK**, Investigation; **BP**, Investigation, **JP**, Investigation; **KK**, Investigation, **SZR**, Investigation **GK**, Investigation; **OD**, Investigation; **GK**, Supervision, Writing – original draft, Writing – review & editing; **GG**, Supervision, Writing – review & editing; **JT**, Supervision, Writing – review & editing; **KZS**, Conceptualization, Funding acquisition, Supervision, Visualization, Writing – original draft, Writing – review & editing.

Declaration of Competing Interest

The authors declare that they have no known competing financial interests or personal relationships that could have appeared to influence the work reported in this paper.

Data Availability

Data will be made available on request.

Acknowledgements

Appendix A. Supporting information

Supplementary data associated with this article can be found in the online version at doi:10.1016/j.envexpbot.2022.105032.

References

Airaki, M., Leterrier, M., Mateos, R.M., et al., 2012. Metabolism of reactive oxygen species and reactive nitrogen species in pepper (Capsicum annuum L.) plants under low temperature stress. Plant Cell Environ. 35, 281–295.

Alloway B.J.,2008. Zinc in Soils and Crop Nutrition. 2nd Edition, IZA and IFA, Brussels, Belgium and Paris, France.

Billard, V., Maillard, A., Garnica, M., Cruz, F., Garcia-Mina, J.M., Yvin, J.C., Ourry, A., Etienne, P., 2015. Zn deficiency in Brassica napus induces Mo and Mn accumulation associated with chloroplast proteins variation without Zn remobilization. Plant Physiol. Biochem. 86, 66–71.

Bradford, M.M., 1976. A rapid and sensitive method for the quantitation of microgram quantities of protein utilizing the principle of protein-dye binding. Anal. Biochem 72, 248–254.

Briat, J., Rouached, H., Tissot, N., Gaymard, F., Dubos, C., 2015. Integration of P, S, Fe and Zn nutrition signals in Arabidopsis thaliana: potential involvement of phosphate starvation response 1 (PHR1). Front Plant Sci. https://doi.org/10.3389/fpls.2015.00290, 6:290.

Broadley, M.R., White, P.J., Hammond, J.P., Zelko, I., Lux, A., 2007. Zinc in plants. New Phytol. 173, 677–702.

Buet, A., Galatro, A., Ramos-Artuso, F., Simontacchi, M., 2019. Nitric oxide and plant mineral nutrition: current knowledge. J. Exp. Bot. 70, 4461–4476.

Cabot, C., Martos, S., Llugany, M., Gallego, B., Tolrà, R., Poschenrieder, C., 2019. A role for zinc in plant defense against pathogens and herbivores, 1664-462X Front Plant Sci. 10. https://doi.org/10.3389/fpls.2019.01171.

Cakmak, I., 2000. Possible roles of zinc in protecting plant cells from damage by reactive oxygen species. N. Phytol. 146, 185–205.

Cakmak, I., 2002. Plant nutrition research: priorities to meet human needs for food in sustainable ways. In: Horst, W.J. (Ed.), Plant Nutrition. Springer, Netherlands, pp. 4–7.

Cakmak, I., Marschner, H., 1988. Enhanced superoxide radical production in roots of zinc-deficient plants. J. Exp. Bot. 39, 1449–1460.

Cakmak, I., Marschner, H., Bangerth, F., 1989. Effect of zinc nutritional status on growth, protein metabolism and levels of indole-3-acetic acid and other phytohormones in bean (Phaseolus vulgaris L.). J. Exp. Bot. 40, 405–412.

Callahan, D.E., Hare, D.J., Bishop, D.P., Doble, P.A., Roessner, U., 2016. Elemental imaging of leaves from the metal hyperaccumulating plant Noccaea caerulescens shows different spatial distribution of Ni, Zn and Cd. RSC Adv. 6, 2337–2344.

Campos, A.C.A., Kruijer, W., Alexander, R., Akkers, R.C., Danku, J., Salt, D.E., Aarts, M. G.M., 2017. Natural variation in Arabidopsis thaliana reveals shoot ionome, biomass, and gene expression changes as biomarkers for zinc deficiency tolerance. J. Exp. Bot. 68, 3643–3656.

Castillo, M., Lozano-Juste, J., González-Guzmán, M., Rodriguez, L., Rodriguez, P.L., León, J., 2015. Inactivation of PYR/PYL/RCAR ABA receptors by tyrosine nitration may enable rapid inhibition of ABA signaling by nitric oxide in plants. Sci. Signal 8: ra89. https://doi.org/10.1126/scisignal.aaa7981.

Chaki, M., Carreras, A., López-Jaramillo, J., Begara-Morales, J.C., Sánchez-Calvo, B., Valderrama, R., Corpas, F.J., Barroso, J.B., 2013. Tyrosine nitration provokes inhibition of sunflower carbonic anhydrase (β-CA) activity under high temperature stress. Nitric Oxide 29, 30–33.

Ciacka, K., Tymiński, M., Gniazdowska, A., Krasuska, U., 2020. Carbonylation of proteins—an element of plant ageing. Planta 252, 12. https://doi.org/10.1007/s00425-020-03414-1.

Corpas, F.J., del Río, L.A., Barroso, J.B., 2007. Need of biomarkers of nitrosative stress in plants. Trends Plant Sci. 12, 436–438.

Corpas, F.J., Carreras, A., Esteban, F.J., Chaki, M., Valderrama, R., del Río, L.A., Barroso, J.B., 2008. Localization of S-nitrosothiols and assay of nitric oxide synthase and S-nitrosoglutathione reductase activity in plants. Methods Enzym. 437, 561–574.

Corpas, F.J., González-Gordo, S., Palma, J.M., 2021. Protein nitration: a connecting bridge between nitric oxide (NO) and plant stress. Plant Stress 2, 100026. https://doi.org/10.1016/j.stress.2021.100026.

Das, S., Green, A., 2013. Importance of zinc in crop and human health. J. SAT Agric. Res. 11, 1–7.

Dhindsa, R.S., Plumb-Dhindsa, P., Thorpe, T.A., 1981. Leaf senescence: correlated with increased levels of membrane permeability and lipid peroxidation, and decreased levels of superoxide dismutase and catalase. J. Exp. Bot. 32, 93–101.

Fancy, N.N., Bahlmann, A.-K., Loake, G.J., 2017. Nitric oxide function in plant abiotic stress. Plant Cell Environ. 40, 462–472.

Feigl, G., Lehotai, N., Molnár, Á., et al., 2015. Zinc induces distinct changes in the metabolism of reactive oxygen and nitrogen species (ROS and RNS) in the roots of two Brassica species with different sensitivity to zinc stress. Ann. Bot. 116, 613–625.

Feigl, G., Varga, V., Molnár, Á., Dimitrakopoulos, P.G., Kolbert Zs, 2020. Different nitro-oxidative response of Odontarrhena lesbiaca plants from geographically separated habitats to excess nickel. Antioxidants 9, 837. https://doi.org/10.3390/antiox9090837.

Ghandilyan, A., Kutman, U.B., Kutman, B.Y., Cakmak, I., Aarts, M.G.M., 2012. Genetic analysis of the effect of zinc deficiency on Arabidopsis growth and mineral concentrations. Plant Soil 361, 227–239.

Gili, B.-N., Sharon, M., 2014. Regulating the 20S proteasome ubiquitin-independent degradation pathway. Biomol 4, 862–884.

Gondor, O.K., Tajti, J., Hamow, K.Á., Majláth, I., Szalai, G., Janda, T., Pál, M., 2021. Polyamine metabolism under different light regimes in wheat. Int. J. Mol. Sci. 22. https://doi.org/10.3390/ijms222111717.

Grewal, H.S., Graham, R.D., 1997. Seed zinc content influences early vegetative growth and zinc uptake in oilseed rape (Brassica napus and Brassica juncea) genotypes on zinc-deficient soil. Plant Soil 192, 191–197.

Grewal, H.S., Stangoulis, J.C.R., Potter, T.D., Graham, R.D., 1997. Zinc efficiency of oilseed rape (Brassica napus and B. juncea) genotypes. Plant Soil 191, 123–132.

Griffith, O.W., 1980. Determination of glutathione and glutathione disulfide using glutathione reductase and 2-vinylpyridine. Anal. Biochem. 106, 207–211.

Guerra, D., Ballard, K., Truebridge, I., Vierling, E., 2016. S-nitrosation of conserved cysteines modulates activity and stability of S-nitrosoglutathione reductase (GSNOR). Biochem 55, 2452–2464.

Hacisalihoglu, G., Kochian, L.V., 2003. How do some plants tolerate low levels of soil zinc? Mechanisms of zinc efficiency in crop plants. N. Phytol. 159, 341–350.

Hänsch, R., Mendel, R.R., 2009. Physiological functions of mineral micronutrients (Cu, Zn, Mn, Fe, Ni, Mo, B, Cl). Curr. Opin. Plant Biol. 12, 259–266.

Haydon, M.J., Kawachi, M., WirtzM, Hillmer, S., Hell, R., Krämer, U., 2012. Vacuolar nicotianamine has critical and distinct roles under iron deficiency and for zinc sequestration in Arabidopsis. Plant Cell 24, 724–737.

He, X., Zhang, H., Ye, X., Hong, J., Ding, G., 2021. Nitrogen assimilation related genes in Brassica napus: Systematic characterization and expression analysis identified hub genes in multiple nutrient stress responses. Plants 10, 2160. https://doi.org/10.3390/plants10102160.

Hess, D.T., Matsumoto, A., Kim, S.O., Marshall, H.E., Stamler, J.S., 2005. Protein S-nitrosylation: purview and parameters. Nat. Rev. Mol. Cell Biol. 6, 150–166.

Höller, S., Meyer, A., Frei, M., 2014. Zinc deficiency differentially affects redox homeostasis of rice genotypes contrasting in ascorbate level. J. Plant Physiol. 171, 1748–1756.

Horák, V., Tròka, I., Stefl, M., 1976. The influence of Zn^{2+} ions on the tryptophan biosynthesis in. Plants V. Biol. Plant 18, 393–396.

Huang, W., Jiao, J., Ru, M., Bai, Z., Yuan, H., Bao, Z., Liang, Z., 2018. Localization and speciation of chromium in Coptis chinensis Franch. using synchrotron radiation X-ray technology and laser ablation ICP-MS. Sci. Rep. 8, 8603. https://doi.org/10.1038/s41598-018-26774-x.

Jahnová, J., Luhová, L., Petřivalský, M., 2019. S-nitrosoglutathione reductase—the master regulator of protein S-nitrosation in plant NO signaling. Plants 8, 48. https://doi.org/10.3390/plants8020048.

Johansson, E., Olsson, O., Nyström, T., 2004. Progression and specificity of protein oxidation in the life cycle of Arabidopsis thaliana. J. Biol. Chem. 279, 22204–22208.

Kolbert, Zs, Feigl, G., Bordé, Á., Molnár, Á., Erdei, L., 2017. Protein tyrosine nitration in plants: present knowledge, computational prediction and future perspectives. Plant Physiol. Biochem 113, 56–63.

Kolbert, Zs, Molnár, Á., Szőllősi, R., Feigl, G., Erdei, L., Ördög, A., 2018. Nitro-oxidative stress correlates with Se tolerance of Astragalus Species. Plant Cell Physiol. 59, 1827–1843.

Kolbert, Zs, Molnár, Á., Oláh, D., Feigl, G., Horváth, E., Erdei, L., Ördög, A., Rudolf, E., Barth, T., Lindermayr, C., 2019. S-nitrosothiol signaling is involved in regulating hydrogen peroxide metabolism of zinc-stressed Arabidopsis. Plant Cell Physiol. 60, 2449–2463.

Kondak, S., Molnár, Á., Oláh, D., Kolbert, Zs, 2022. The role of nitric oxide (NO) in plant responses to disturbed plant zinc homeostasis. Plant Stress 4, 100068. https://doi.org/10.1016/j.stress.2022.100068.

Kovács, I., Holzmeister, C., Wirtz, M., et al., 2016. ROS-mediated inhibition of S-nitrosoglutathione reductase contributes to the activation of anti-oxidative mechanisms. Front Plant Sci. 7, 1669. https://doi.org/10.3389/fpls.2016.01669.

Kubienova, L., Kopecny, D., Tylichova, M., et al., 2013. Structural and functional characterization of a plant S-nitrosoglutathione reductase from Solanum lycopersicum. Biochimie 95, 889–902.

Kumar, D., Yusuf, M.A., Singh, P., Sardar, M., Sarin, N.B., 2014. Histochemical detection of superoxide and H2O2 accumulation in Brassica juncea Seedlings. Bio Protoc. 4, e1108 https://doi.org/10.21769/BioProtoc.1108.

Law, M.Y., Charles, S.A., Halliwell, B., 1983. Glutathione and ascorbic acid in spinach (Spinacia oleracea) chloroplasts. The effect of hydrogen peroxide and of Paraquat. Biochem J. 210, 899–903.

Lilay, G.H., Persson, D.P., Castro, P.H., Liao, F., Alexander, R.D., Aarts, M.G.M., Assunção, A.G.L., 2021. Arabidopsis bZIP19 and bZIP23 act as zinc sensors to control plant zinc status. Nat. Plants 7, 137–143.

Limbeck, A., Brunnbauer, L., Lohninger, H., Porízka, P., Modlitbova, P., Kaiser, J., Janovszky, P., Kéri, A., Galbács, G., 2021. Methodology and applications of elemental mapping by laser induced breakdown spectroscopy. Anal. Chim. Acta 1147, 72–98.

Lindermayr, C., 2018. Crosstalk between reactive oxygen species and nitric oxide in plants: Key role of S-nitrosoglutathione reductase. Free Radic. Biol. Med 122, 110–115.

Mano, Y., Nemoto, K., 2012. The pathway of auxin biosynthesis in plants. J. Exp. Bot. 63, 2853–2872.

Marschner, P., 2012. Marschner's Mineral Nutrition of Higher Plants, Third ed. Academic Press. https://doi.org/10.1016/C2009-0-63043-9.

Martinez, M.C., Achkor, H., Persson, B., et al., 1996. Arabidopsis formaldehyde dehydrogenase. Molecular properties of plant class III alcohol dehydrogenase provide further insights into the origins, structure and function of plant class p and liver class I alcohol dehydrogenases. Eur. J. Biochem. 241, 849–857.

McRae, R., Bagchi, P., Sumalekshmy, S., Fahrni, C.J., 2009. In situ imaging of metals in cells and tissues. Chem. Rev. 109, 4780–4827.

Neill, S., Bright, J., Desikan, D., HancockJ, Harrison, J., Wilson, I., 2008. Nitric oxide evolution and perception. J. Exp. Bot. 59, 25–35.

Noulas, C., Tziouvalekas, M., Karyotis, T., 2018. Zinc in soils, water and food crops. J. Trace Elem. Med. Biol. 49, 252–260.

Nystrom, T., 2005. Role of oxidative carbonylation in protein quality control and senescence. EMBO J. 24, 1311–1317.

Pandey, N., Gupta, B., Pathak, G.C., 2012. Antioxidant responses of pea genotypes to zinc deficiency. Russ. J. Plant Physiol. 59, 198–205.

Paradisone, V., Navarro-León, E., Ruiz, J.M., Esposito, S., Blasco, B., 2021. Calcium silicate ameliorates zinc deficiency and toxicity symptoms in barley plants through improvements in nitrogen metabolism and photosynthesis. Acta Physiol. Plant 43, 154. https://doi.org/10.1007/s11738-021-03325-y.

Pinton, R., Cakmak, I., Marschner, H., 1994. Zinc defciency enhanced NAD(P)H-dependent superoxide radical production in plasma membrane vesicles isolated from roots of bean plants. J. Exp. Bot. 45, 45–50.

Rose, M.T., Rose, T.J., Pariasca-Tanaka, J., Yoshihashi, T., Neuweg, H., 2012. Root metabolic response of rice (Oryza sativa L.) genotypes with contrasting tolerance to zinc deficiency and bicarbonate excess. Planta 236, 959–973.

Saenchai, C., Bouain, N., Kisko, M., Prom-u-thai, C., Doumas, P., Rouached, H., 2016. The involvement of OsPHO1;1 in the regulation of iron transport through integration of phosphate and zinc deficiency signaling. Front Plant Sci. 7, 396. https://doi.org/10.3389/fpls.2016.00396.

Sakamoto, A., Ueda, M., Morikawa, H., 2002. Arabidopsis glutathione-dependent formaldehyde dehydrogenase is an S-nitrosoglutathione reductase. FEBS Lett. 515, 20–24.

Sakamoto, T., Kamiya, T., Sako, K., Yamaguchi, J., Yamagami, M., Fujiwara, T., 2011. Arabidopsis thaliana 26S proteasome subunits RPT2a and RPT5a are crucial for zinc deficiency-tolerance. Biosci. Biotechol. Biochem. 75, 561–567.

Sarret, G., Harada, E., Choi, Y.-E., et al., 2006. Trichomes of tobacco excrete zinc as zinc-substituted calcium carbonate and other zinc-containing compounds. Plant Physiol. 141, 1021–1034.

Seethambaram, Y., Das, V.S.R., 1986. Effect of zinc defciency on enzyme activities of nitrate reduction and ammonia assimilation of Oryza sativa L. and Pennisetum americanum L. Leeke. Proc. Indian Natl. Sci. Acad. 4, 491–496.

Shanmugam, V., Tsednee, M., Yeh, K.-C., 2012. Zinc tolerance induced by iron 1 reveals the importance of glutathione in the cross-homeostasis between zinc and iron in Arabidopsis thaliana. Plant J. 69 (6), 1006–1017.

Sharma, P.N., Kumar, P., Tewari, R.K., 2004. Early signs of oxidative stress in wheat plants subjected to zinc deficiency. J. Plant Nutr. 27, 451–463.

Shinozaki, D., Merkulova, E.A., Naya, L., et al., 2020. Autophagy increases zinc bioavailability to avoid light-mediated reactive oxygen species production under zinc deficiency. Plant Physiol. 182, 1284–1296.

Signorelli, S., Corpas, F.J., Borsani, O., Barroso, J.B., Monza, J., 2013. Water stress induces a differential and spatially distributed nitro-oxidative stress response in roots and leaves of Lotus japonicus. Plant Sci. 201–202, 137–146.

Stasolla, C., Huang, S., Hill, R.D., Igamberdiev, A.U., 2019. Spatio-temporal expression of phytoglobin: a determining factor in the NO specification of cell fate. J. Exp. Bot. 70, 4365–4377.

Tanou, G., Filippou, P., Belghazi, B., Job, D., Diamantidis, G., Fotopoulos, V., Molassiotis, A., 2012. Oxidative and nitrosative-based signaling and associated post-translational modifications orchestrate the acclimation of citrus plants to salinity stress. Plant J. 72, 585–599.

Tewari, R.K., Kumar, P., Sharma, P.N., 2019. An effective antioxidant defense provides protection against zinc deficiency-induced oxidative stress in Zn-efficient maize plants. J. Plant Nutr. Soil Sci. 182, 701–707.

Thiébaut, N., Hanikenne, M., 2022. Zinc deficiency responses: bridging the gap between Arabidopsis and dicotyledonous crops. J. Exp. Bot. 73, 1699–1716.

Tichá, T., Činčalová, L., Kopečný, D., Sedlářová, M., Kopečná, M., Luhová, L., Petřivalský, M., 2017a. Characterization of S-nitrosoglutathione reductase from Brassica and Lactuca spp. and its modulation during plant development. Nitric Oxide 68, 68–76.

Tichá, T., Lochman, J., Činčalová, L., Luhová, L., Petřivalský, M., 2017b. Redox regulation of plant S-nitrosoglutathione reductase activity through post-translational modifications of cysteine residues. Biochem. Biophys. Res. Commun. 494, 27–33.

Tola, A.J., Amal Jaballi, A., Missihoun, T.D., 2021. Protein carbonylation: emerging roles in plant redox biology and future prospects. Plants 10, 1451. https://doi.org/10.3390/plants10071451.

Ullah, A., Romdhane, L., Rehman, A., Farooq, M., 2019. Adequate zinc nutrition improves the tolerance against drought and heat stresses in chickpea. Plant Physiol. Biochem 143, 11–18.

Umbreen, S., Lubega, J., Cui, B., Pan, Q., Jiang, J., Loake, G.J., 2018. Specificity in nitric oxide signalling. J. Exp. Bot. 69, 3439–3448.

Ventimiglia, L., Mutus, B., 2020. The physiological implications of S-nitrosoglutathione reductase (GSNOR) activity mediating NO signalling in plant root structures. Antiox 9, 1206. https://doi.org/10.3390/antiox9121206.

Wang, H., Jin, J., 2007. Effects of zinc deficiency and drought on plant growth and metabolism of reactive oxygen species in maize (Zea mays L). Agric. Sci. China 6, 988–995.

Wang, J., Moeen-ud-din, M., Yang, S., 2021. Dose-dependent responses of Arabidopsis thaliana to zinc are mediated by auxin homeostasis and transport. Environ. Exp. Bot. 189, 104554 https://doi.org/10.1016/j.envexpbot.2021.104554.

Welinder, C., Ekblad, L., 2011. Coomassie staining as loading control in Western blot analysis. J. Proteome Res. 10, 1416–1419.

Wu, B., Zoriy, M., Chen, Y., Becker, J.S., 2009a. Imaging of nutrient elements in the leaves of Elsholtzia splendens by laser ablation inductively coupled plasma mass spectrometry (LA-ICP-MS). Talanta 78, 132–137.

Wu, B., Chen, Y., Becker, J.S., 2009b. Study of essential element accumulation in the leaves of a Cu-tolerant plant Elsholtzia splendens after Cu treatment by imaging laser ablation inductively coupled plasma mass spectrometry (LA-ICP-MS). Anal. Chim. Acta 633, 165–172.

Ye, J., Coulouris, G., Zaretskaya, I., Cutcutache, I., Rozen, S., Madden, T., 2012. Primer-BLAST: a tool to design target-specific primers for polymerase chain reaction. BMC Bioinform. 13, 134. https://doi.org/10.1186/1471-2105-13-134.

Zeng, H., Zhang, X., Ding, M., Zhu, Y., 2019a. Integrated analyses of miRNAome and transcriptome reveal zinc deficiency responses in rice seedlings. BMC Plant Biol. 19, 585. https://doi.org/10.1186/s12870-019-2203-2.

Zeng, H., Zhang, X., Ding, M., Zhang, X., Zhu, Y., 2019b. Transcriptome profiles of soybean leaves and roots in response to zinc deficiency. Physiol. Plant 167, 330–351.

Zeng, H., Wu, H., Yan, F., Yi, K., Zhu, Y., 2021. Molecular regulation of zinc deficiency responses in plants. J. Plant Physiol. 261, 153419 https://doi.org/10.1016/j.jplph.2021.153419.